CHAPTER IV

RESULTS AND DISCUSSIONS

4.1 Caffeic acid derivatives synthesis

In this study 4 ester and 4 amide derivatives of CAF were synthesized and grouped according to their functional groups and side chain groups. The FT-IR, ^{1}H-NMR, ^{13}C –NMR and MS spectrums of CAF ester and amide derivatives are shown in Appendix B and details of each derivative are shown below.

1. Ethyl 1-(3',4'-dihydroxyphenyl) propenate, EDP

Yield: 60%. m.p: 149-151 °C (colourless powder); **FT-IR** ν_{max} (KBr): 3468.75, 3375.05, 2953.12, 2890.62, 1679.69, 1640.62, 1589.06; **H^{1}-NMR**(400 MHz, acetone –d6); δ: 8.21 (2H, br s), 7.46 (1H,d, *J*=16.1 Hz), 7.11 (1H,d, *J*=2.0 Hz) 7.03 (1H,dd, *J*=2.0, 8.3 Hz), 6.87 (1H, d, *J*=7.8 Hz), 6.27 (1H,d, *J*=16.1 Hz), 4.17 (2H,q, *J*=7.3 Hz), 1.25 (3H,t, *J*=7.3 Hz); **C13-NMR**: 126.2, 114.6, 144.1 146.6, 114.3, 121.1, 144.25, 114.4, 166.4, 59.3, 13.5; **MS** *m/z*: 208 (100%, M^{+}), 180, 163, 145, 117, 89

The EDP structure is shown in Fig 4.1

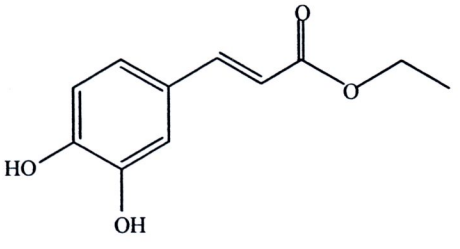

Fig. 4.1 The structure of EDP

2. Octyl 1-(3',4'-dihydroxyphenyl) propenate, ODP

Yield: 45%, mp: 110-111°C (colourless powder); **FT-IR ν_{max} (KBr):** 3487.62, 3328.14, 2917.95, 2832.52, 1682.66, 1599.07, 1523.22; **H^1-NMR**(400 MHz, acetone –d6): 8.41 (1H,s), 8.13 (1H,s), 7.54 (1H,d, *J*=16.1 Hz), 7.15 (1H,d, *J*=2.0 Hz), 7.03 (1H, dd, *J*=2.0, 8.1 Hz), 6.86 (1H,d, *J*=8.1 Hz , 6.28 (1H,d, *J*=16.0 Hz), 4.13(2H,t, *J*=6.7 Hz), 1.66 (2H,quint, *J*=6.7 Hz), 1.45-1.14 (10H,m), 0.86 (3H,t, *J*=6.9 Hz); **C13- NMR**: 167.3, 146.7, 145, 144.24, 126.4, 121.2, 114.7, 114.6, 113.4, 63.8, 32, 31.3, 25.6, 24.7, 24, 22.2, 13.5; **MS** *m/z*: 292 (M^+), 193, 180 (100%), 163, 117. The structure of ODP is shown in Fig. 4.2

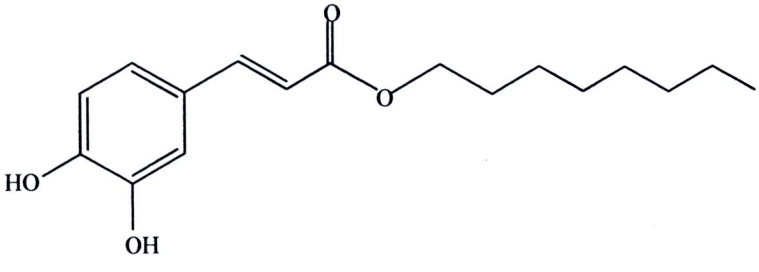

Fig. 4.2 The structure of ODP

3. Phenylmethyl 1-(3',4'-dihydroxyphenyl) propenate, PMDP

Yield: 40% m.p 153-155°C colourless powder; **FT-IR** ν_{max} (KBr): 3406.25, 3335.92, 1687.50, 1640.62, 1593.75, 1515.63; **H^1-NMR**(400 MHz, acetone –d6): 8.31 (2H, br s), 7.58 (1H, d, J = 15.8 Hz), 7.45–7.28 (5H, m), 7.17 (1H, d, J = 2.1 Hz), 7.07, 7.06(1H, dd, J = 2.1, 8.1 Hz), 6.86 (1H, d, J = 8.1 Hz), 6.34 (1H, d,J = 16.0 Hz), 5.21 (2H, s); **C13-NMR**: 167.2, 166.1, 146.8, 146.7, 144.2, 135.8, 128, 126.11, 125.99, 114.6; **MS** *m/z*: 270 (M+, 100%), 225, 207, 177, 147, 121, 105, 79.

The structure of PMDP is shown in Fig 4.3

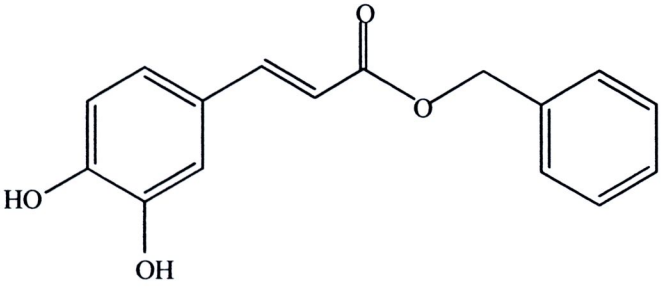

Fig. 4.3 The structure of PMDP

4. Phenylethyl 1-(3',4'-dihydroxyphenyl) propenate, PEDP

Yield: 47% mp 153-155°C colourless powder; **FT-IR** ν_{max} (KBr): 3439.0, 3317.19, 2909.37, 2851.56, 1632.81, 1601.56, 1531.25, 1054.68; **H^1-NMR**(400 MHz, acetone –d6); 7.58 (1H,d, J = 15.8 Hz), 7.26-7.40 (5H, m), 7.06 (1H,d, J = 2.1 Hz), 6.93 (1H,dd, J = 2.1, 8.1 Hz), 6.79 (1H,d, J = 8.1 Hz), 6.30 (1H,d, J = 15.8 Hz) ,5.19 (2H,s), 5.04 (2H,broad); **C^{13}-NMR**; 169.0, 149.5, 147.1, 146.7, 137.7, 129.5, 129.1, 127.7, 123.0, 116.5, 115.2, 114.9, 67.1; **MS** (*m/z*): 284(M^+), 181, 149, 135 (100%), 99

The PEDP structure is shown in Fig 4.4.

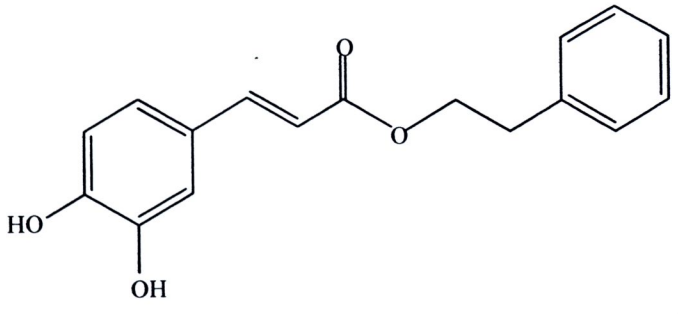

Fig. 4.4 The structure of PEDP

5. Ethyl 1-(3', 4'-dihydroxyphenyl) propenamide, EDPA

Yield: 36.25 % mp 153-155°C colourless powder; **FT-IR** ν_{max} (KBr): 3476.56, 3296.88, 1679, 1640, 1609, 1100; H^1-NMR(400 MHz, acetone –d6); 8.3 (2H, br s), 7.6 (1H,s, *J*=16.1 Hz), 7.12 (1H,d, *J*=2.0 Hz), 6.97(1H,dd, *J*=2.0, 8.3 Hz), 6.6 (1H, d, *J*=7.8 Hz), 6.23 (1H,d, *J*=16.1 Hz), 4.23 (2H,q, *J*=7.3 Hz), 1.34 (3H,t, *J*=7.3 Hz)

C^{13}-NMR: 126.3, 114.7, 144.3, 146.6, 113.4, 121.2, 144.1, 114.5, 166.7, 59.5, 13.7; **MS** (*m/z*): 207 (M^+, 100%), 163, 132, 75, 43. The EDPA structure is shown in Fig. 4.5.

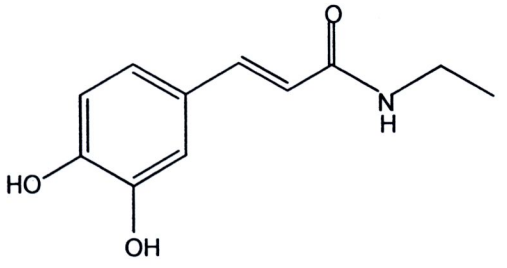

Fig. 4.5 The structure of EDPA

6. Octyl 1-(3', 4'-dihydroxyphenyl) propen amide, ODPA

Yield: 30.45 % mp 119-121°C colourless powder; **FT-IR** ν_{max} (KBr): 3421.88, 3262.5, 1632.8, 1601.0, 1652.25, 1492.0, 1437.0, 1218.0; **H^1-NMR**(400 MHz, acetone –d6);7.14 (d, J=14 Hz, 1H), 6.7-7.1 (m, 3H), 6.3 (d, J=14 Hz), 3.3 (m, 2H), 1.0-1.7 (m, 17H); **C^{13}-NMR**: 167.3, 146.7, 145, 144.24, 126.4, 121.2, 114.7, 114.6, 113.4, 63.8, 32, 31.3, 25.6, 24.7, 24, 22.2, 13.5; **MS** (*m/z*): 291 (M^+), 207 (100%), 177, 134, 91. The structure of ODPA is shown in Fig. 4.6

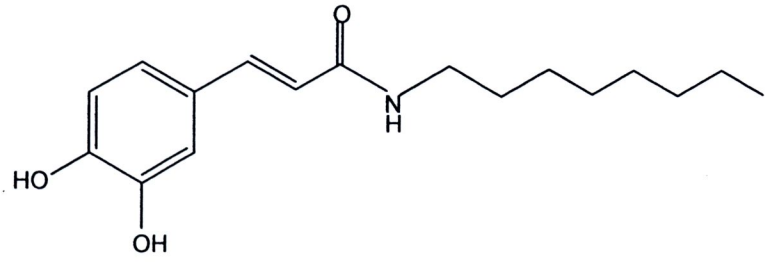

Fig. 4.6 The structure of ODPA

7. Phenmethyl 1-(3', 4'-dihydroxyphenyl) propen amide, PMDPA

Yield: 45.80 % colourless powder; FT-IR ν_{max} (KBr): 3421.88, 3262.5, 1632.8, 1601.0, 1652.25, 1492.0, 1437.0, 1218.0; **H^1-NMR**(400 MHz, acetone –d6); 2.83 (s, 3H), 6.20 (d, J=20 Hz,1H), 6.70-7.00 (m, 3H), 7.30 (d, J=20 Hz, 1H0, 6.43 (d, J=22 Hz, 1H), 6.80-7.70 (m, 8H), 7.53 (d, J=22 Hz, 1H), 8.24 (s, 1 H); **C^{13}-NMR**: 167.2, 166.1, 146.8, 146.7, 144.2, 135.8, 128, 126.11, 125.99, 114.6; **MS** (*m/z*): 269 (M^+), 209 (100%), 180, 164, 133, 109, 79. The structure of PMDPA is shown in Fig. 4.7

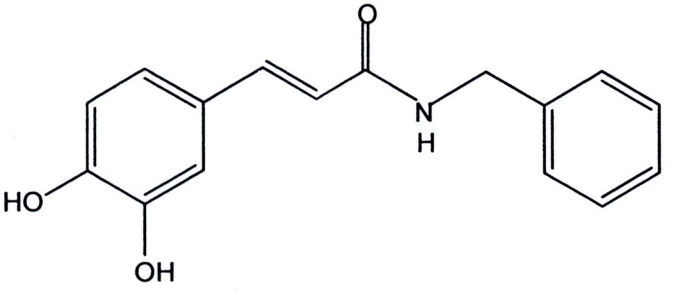

Fig. 4.7 The structure of PMDPA

8. Phenethyl 1-(3', 4'-dihydroxyphenyl) propen amide ,PEDPA

Yield: 24.60 % colourless powder; **FT-IR** ν_{max} (KBr): 3421.88, 3262.5, 1632.8, 1601, 1652.25, 1492, 1437, 1218; **H^1-NMR**(400 MHz, acetone –d6): 2.83 (t, J=7.8, 2H), 3.51 (dd, J= 5.9, 2H), 6.43 (d, J=15.6), 6.81 (d, J=8.3, 1H), 6.90 (dd, J=2.0, J=7.81, 1H), 7.06 (d, J=20 Hz, 1H), 7.20-7.26 (m, 5H), 7.3 (s, 1H), 7.41 (d, J=15.6 Hz, 1H), 8.3 (s, H); **C^{13}-NMR**: 169.0, 149.5, 147.1, 146.7, 137.7, 129.5, 129.1, 127.7, 123.0, 116.5, 115.2, 114.9, 67.1; **MS** (*m/z*): 283(M^+), 265, 207 (100%), 134, 97, 75. The structure of ODPA is shown in Fig. 4.8

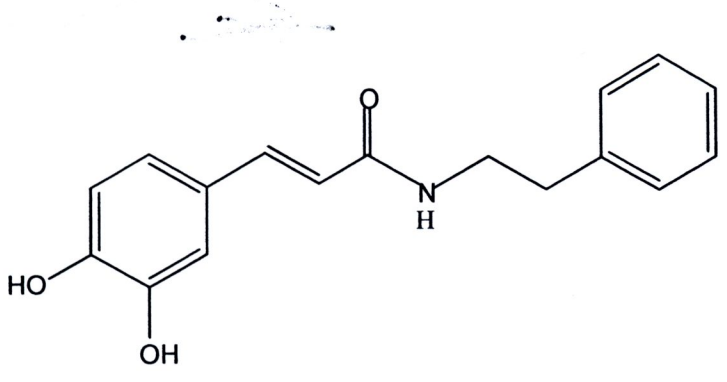

Fig. 4.8 The structure of PEDPA

4.2. Free radical scavenging and antioxidant properties of caffeic acid and its derivatives

4.2.1 DPPH radical scavenging activity

DPPH is a stable nitrogen free radical compound that has been used to determine the free radical-scavenging ability of samples [73]. DPPH• assay is the simplest method for measuring the antiradical ability. The scavenging effects of CAF and its amide and ester derivatives along with those of ascorbic acid and α-tocopherol, serve as positive controls, are presented in Fig 4.9a and 4.9b. The CAF and its derivatives showed a variation of IC_{50} values ranging from 61.32- 878.12 μg/ml and the IC_{50} values presented in table 4.1. The EDPA was found to have the most powerful DPPH radical scavenging activity, as evidenced by the lowest IC_{50} value. The scavenging activity of DPPH radicals decreased in the following order: EDPA> EDP> CAF> ODP> PMDPA> ODPA> PMDP> PEDP> PEDPA. The result showed that the smaller CAF derivatives molecules, the higher potential in DPPH radical scavenging activity. The different in radical scavenging activity between EDPA and EDP may be due to the amide bond which is highly stable than the ester bond [74].

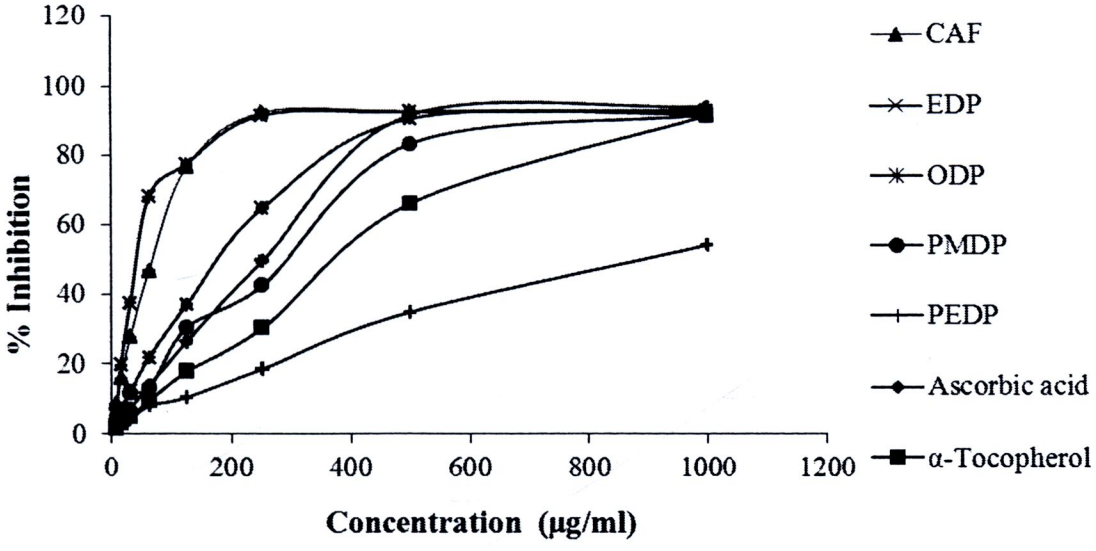

Fig. 4.9a DPPH radical scavenging ability of CAF and its ester derivatives

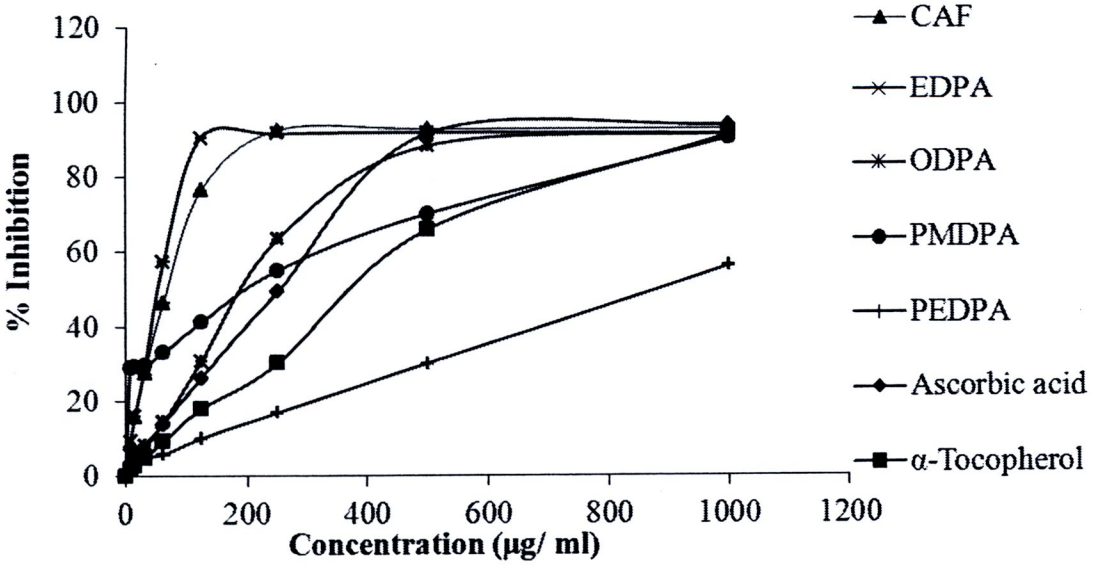

Fig 4.9b DPPH radical scavenging ability of CAF and its amide derivatives

4.2.2. Hydroxyl radical scavenging activities

Hydroxyl radical is an extremely reactive oxygen species, capable of modifying almost macromolecule in the living cells. This radical has the capacity to cause DNA damage leading to carcinogenesis, mutagenesis and cytotoxicity. Furthermore, hydroxyl radicals are prompt to initiate lipid oxidation process [75]. Due to high reactivity of hydroxyl radicals, measurements based on scavenging hydroxyl radicals are not accurate. Deoxyribose assay performed in the absence of EDTA (site-specific model), forms hydroxyl radicals on the surface of the ribose substrate in the presence of hydrogen peroxide and ascorbic acid. In this model, the only substrate that inhibit deoxyribose degradation are those that bind iron strongly enough to remove them from deoxyribose and form complex less reactive in generating hydroxyl radicals [76]. Fig. 4.10a and 4.10b show the ability of CAF and its derivatives at different concentrations to scavenge hydroxyl radical compared with ascorbic acid and α- tocopherol as positive controls. The IC_{50} values are shown in Table 4.1. CAF and it derivatives possess highly hydroxyl radical scavenging with similarly IC_{50} value, 4 ng/ ml. Biologically, the hydroxyl radical is widely generated by Fenton reaction [77]. This study showed that CAF and its derivatives are promising compounds to scavenge hydroxyl radical *in vitro*. Further study using *in vivo* model, toxicity testing and evaluation for adverse effects should be carried out.

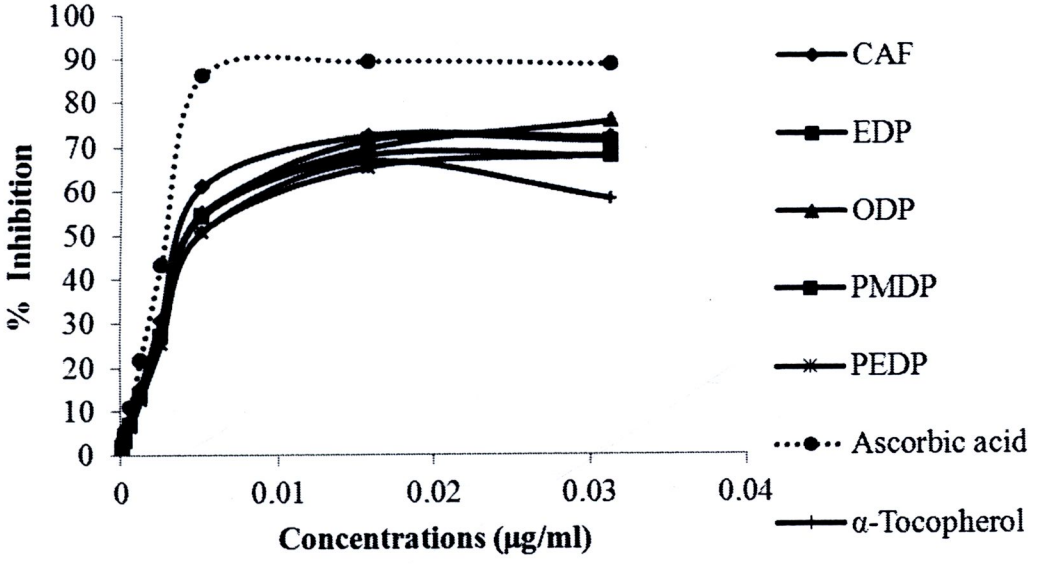

Fig. 4.10a Percent inhibition of CAF and its ester derivatives on scavenging hydroxyl radical

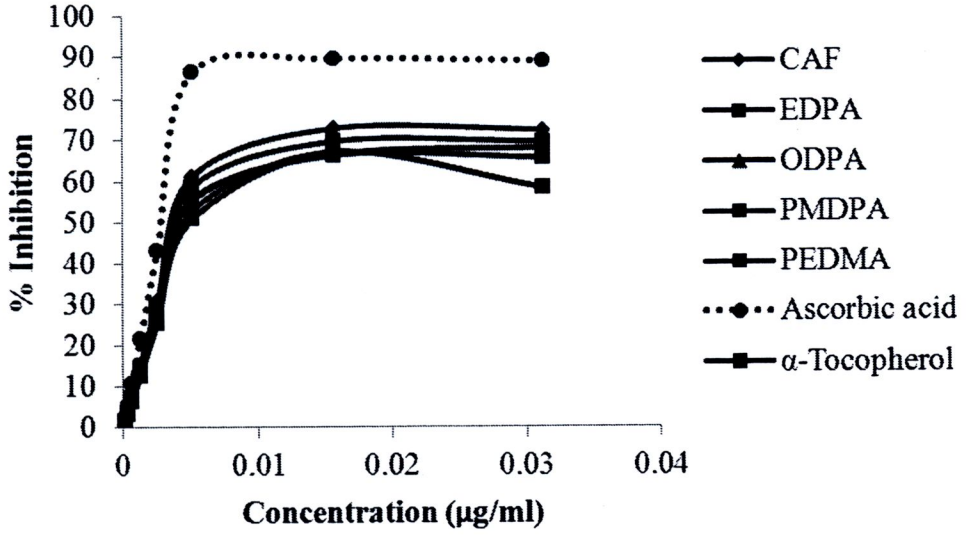

Fig. 4.10b Percent inhibition of CAF and its amide derivatives on scavenging hydroxyl radical.

4.2.3. Ferric reducing antioxidant power (FRAP)

FRAP is based on the ability of antioxidant power to reduce Fe^{3+} to Fe^{2+} in the presence of TPTZ, forming an intense blue of Fe^{2+}-TPTZ complex with a maximum absorbance at 593 nm. The reaction is pH-dependent (optimum pH 3.6). The decrease of absorbance is proportional to the antioxidant ability [78]. In the present study, the trend for ferric ion reducing activities of CAF and its derivatives are shown in Fig 4.11 a and 4.11b. The absorbance of CAF and EDPA were increasing and constant at 500-1000 μg/ml. For other derivatives, the absorbance clearly increased, due to the formation of the Fe^{2+}-TPTZ complex with increasing concentration.

Being expressed in $FeSO_4$ equivalents, the FRAP value was applied, to determine the antioxidant ability of CAF, synthesized substances and standards. The highest reducing activity belongs to CAF, compared with other derivatives and natural antioxidant, ascorbic acid and α-tocopherol. Similar to the results obtained from the DPPH assay, CAF and EDPA showed relatively strong ferric ion-reducing activities. PEDP and PEDPA showed lower ferric ion-reducing activities. This result suggests that the smaller molecule of the derivatives, the stronger ferric ion- reducing activity.

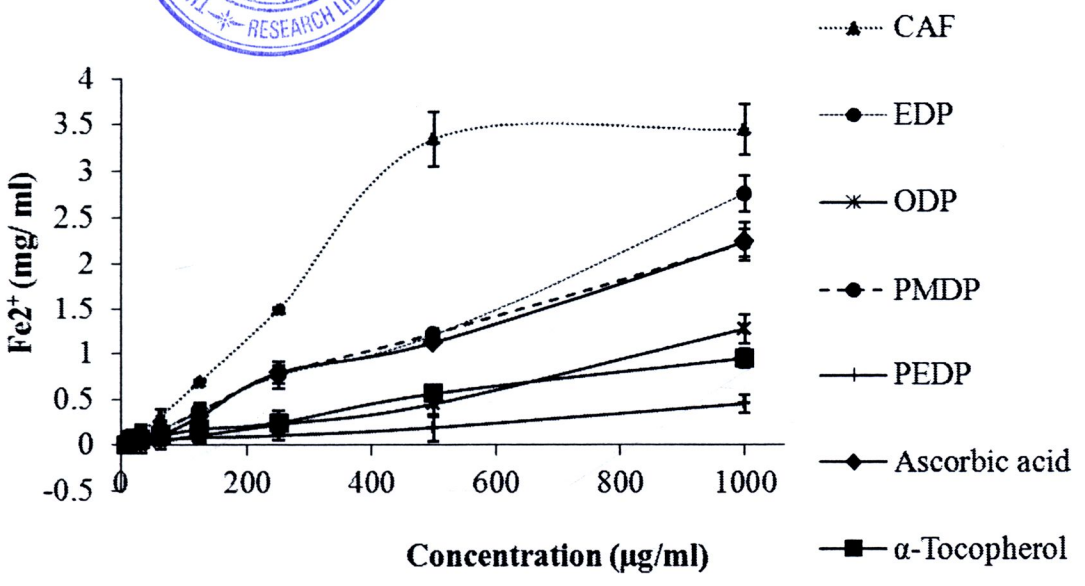

Fig 4.11a Ferric reducing antioxidant power of CAF and its ester derivatives.

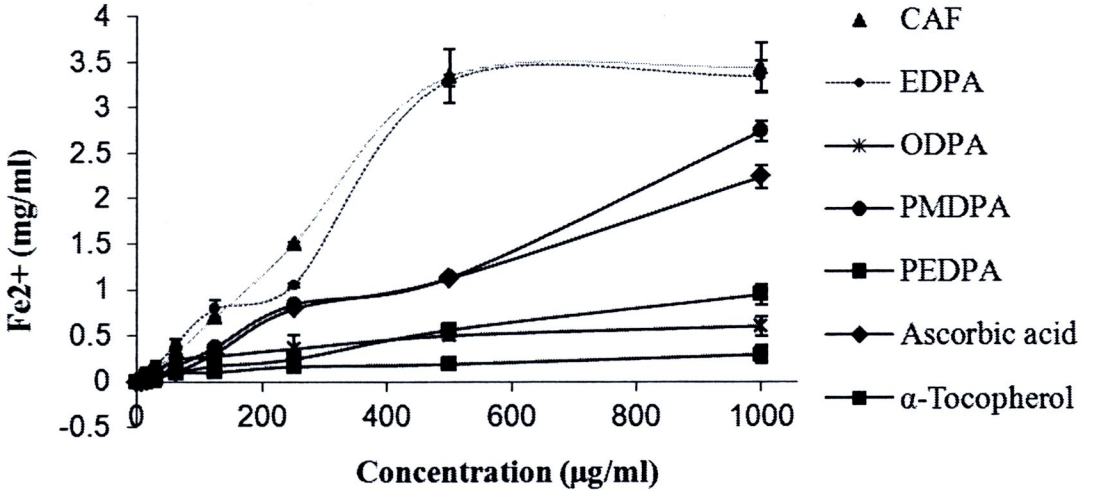

Fig. 4.11b. Ferric reducing antioxidant power of CAF and its amide derivatives.

4.2.4. Reducing power

Reducing power assay is used to determine the ability of natural antioxidant to donate electron [79]. Many reports have revealed that there is a direct correlation between antioxidant activities and reducing power of substances [80]. Fig. 4.12a and 4.12b show the reducing power which indicate by increasing of absorbance at 700 nm. Reducing power of ester and amide derivatives were compared with CAF, ascorbic acid and α-tocopherol. The reducing power of all samples increased in dose-dependent manner. The reducing power of CAF and its derivatives at 250 μg/ ml is shown in Table 4.1. According to the results in the present study, it suggested that the reducing powers of amide derivatives are greater than those of ester derivatives because amide derivatives can donate three hydrogen atoms while ester derivatives can donate only two electrons. The smaller molecules, the greater reducing power.

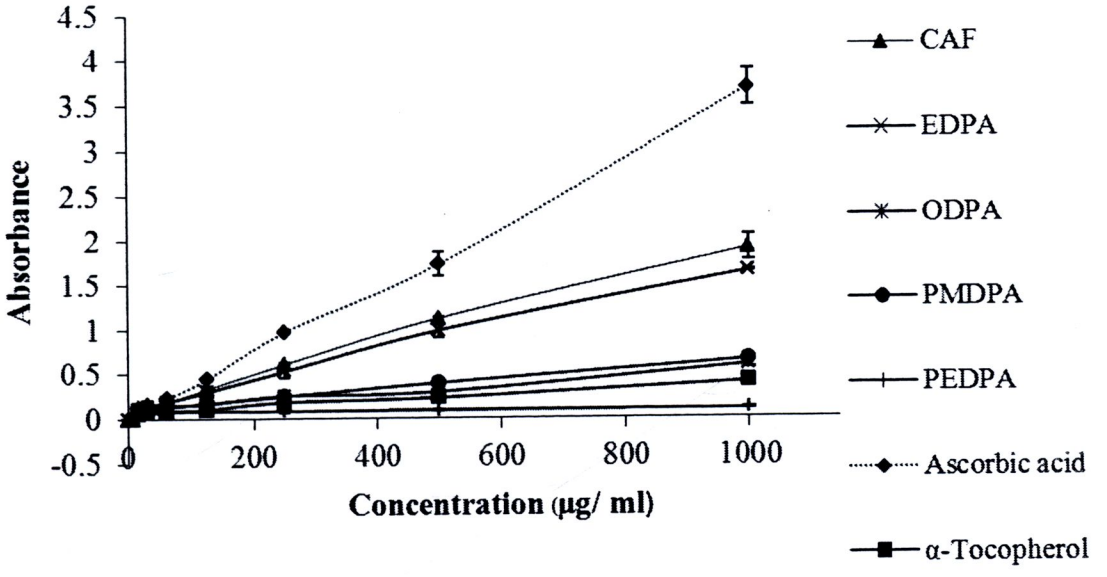

Fig. 4.12a Reducing power of CAF and its ester derivatives

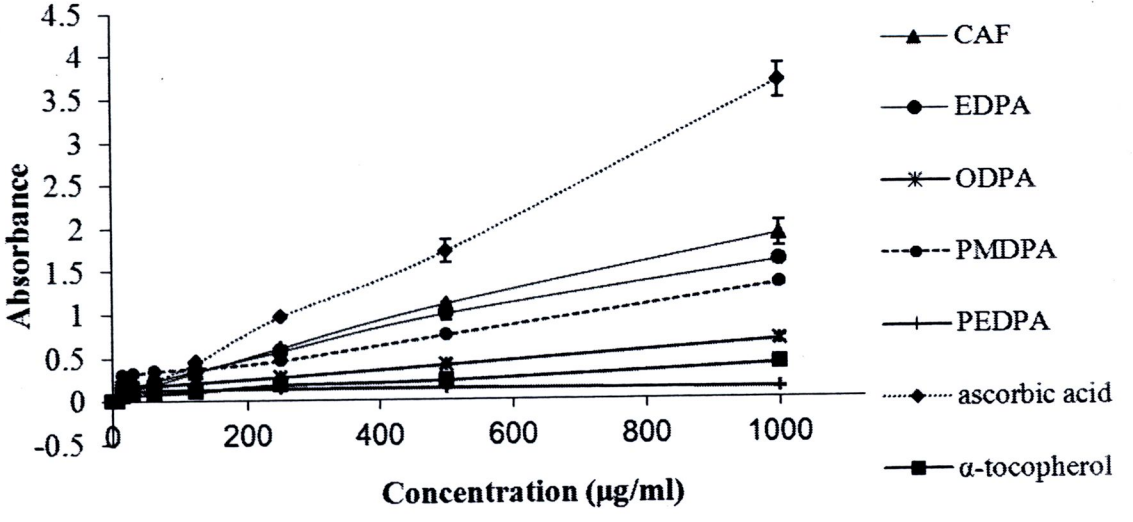

Fig.4.12b Reducing power of CAF and its amide derivatives

4.2.5. Superoxide anion radical scavenging

Superoxide is the one electron reduced from the oxygen molecule which produced by activated phagocytes and xenobiotic biotransformation. It is a precursor of hydrogen peroxide, hydroxyl radical and singlet oxygen that have the potential to react with macromolecules and induce tissue damage [81]. In the PMS-NADPH-NBT system, superoxide anion produced from dissolved oxygen from the coupling reaction of PMS-NADPH that reduced NBT. The decrease in absorbance at 560 nm with antioxidants indicates the consumption of superoxide anion in the reaction mixture [82]. Fig. 4.6a and 4.6b shows the ability of CAF and it derivatives to inhibit superoxide radical generation when using ascorbic acid and α-tocopherol as positive controls. The CAF and its derivatives demonstrated a concentration-dependent scavenging ability by neutralizing superoxide radicals. The IC_{50} values of them are shown in Table 4.1. The rank of potency in superoxide anion scavenging was EDP > EDPA> CAF> PEDP> PMDPA> ODPA> PMDP > ODP> PMDPA.

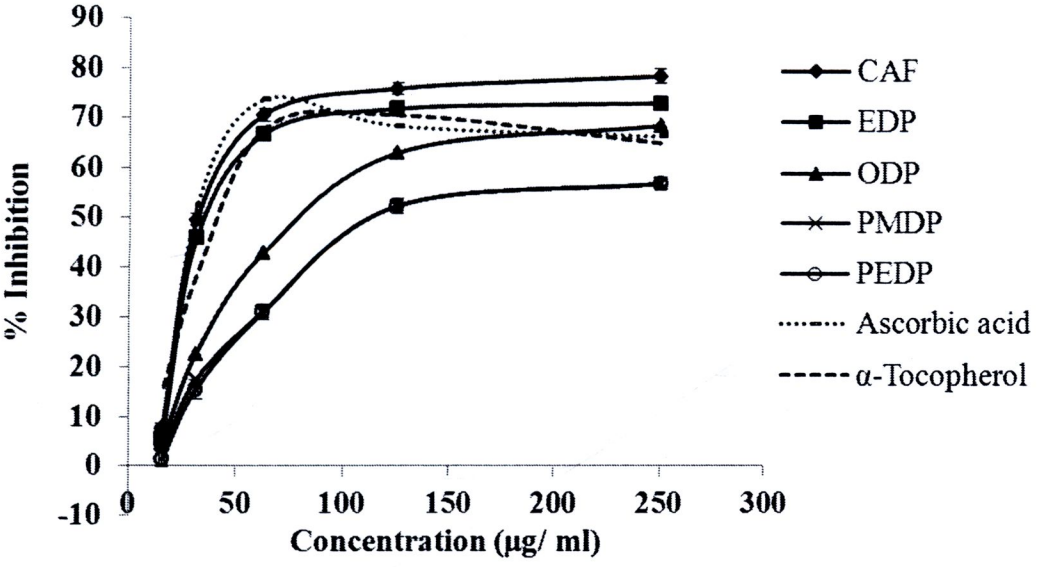

Fig. 4.13a Percent inhibition of CAF and its ester derivatives on superoxide anion generation.

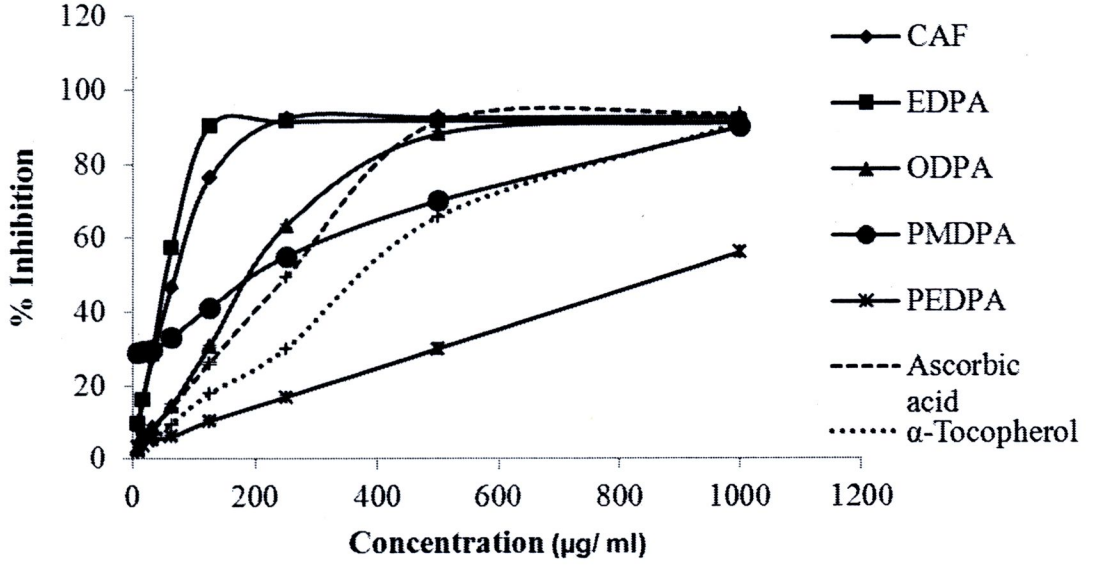

Fig. 4.13b Percent inhibition of CAF and its amide derivatives on superoxide anion generation

4.2.6. Nitric oxide radical scavenging

Nitric oxide (NO) is an important chemical produced by macrophages, endothelial cells and neurons and is involved in the regulation of various physiological processes. Excess NO concentration is associated with several diseases. Moreover, NO can react with superoxide to form the peroxynitrite anion, which is a potential strong oxidant that can decompose to hydroxyl radical and nitrous oxide [83]. Recent studies have shown that reactive nitrogen intermediates play an important role in inflammatory process and carcinogenic process [84]. Fig 4.13a and 4.13b present the NO-scavenging effects of tested CAF and its derivatives. All derivatives had NO-scavenging activity dose-dependently ranging from 19-149 μg/mL. The IC_{50} values for NO-scavenging ability were calculated from the linear equation. The CAF possessed the highest scavenging potency. The order of potency considering from IC_{50} values was CAF> EDP> ODP> EDPA> PMDP> PMDPA> ODPA. The IC 50 values of CAF and its derivatives are shown in Table 4.1. The IC_{50} value of PEDP was higher than 1,000 μg/ml because CAF esters were not stable molecule and labile in biological fluids [85]. The results show that the smaller ester derivatives of CAF, the higher NO-scavenging activity due to its hydrophobic properties.

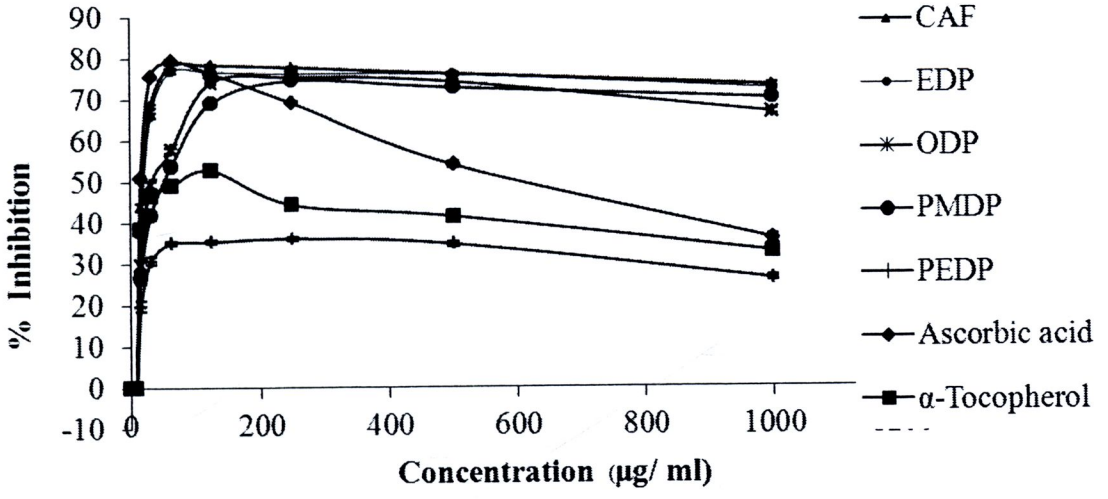

Fig. 4.14a Percent inhibition of CAF ester on nitric oxide generation.

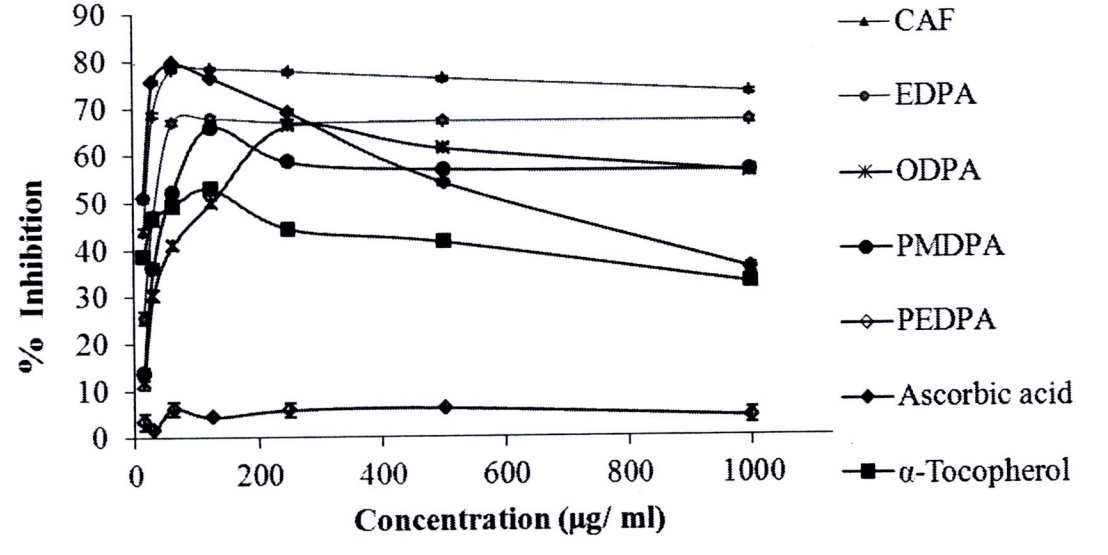

Fig. 4.14b Percent inhibition of CAF amide on nitric oxide generation.

4.2.7 Antioxidant activity in linoleic acid emulsion system

Biomolecule such as lipid, protein and DNA are the target sites of free radical damage in the living cells. Therefore, a potential antioxidant *in vivo* should have inhibitory effects against lipid peroxidation and membrane damage. Linoleic acid is fatty acid containing in cell membrane and therefore is used to study lipid oxidation. AAPH is water soluble and the generation rate of free radicals from the decomposition of AAPH can be easily controlled and measured [86]. In this study, AAPH-induced linoleic acid peroxidation was used for study of inhibitory effect of CAF and its derivatives on lipid peroxidation. The peroxidation was initiated by AAPH that could decompose at physiological temperature and generate alkyl radicals to initiate lipid peroxidation. Percent of inhibition of the conjugated diene formation during linoleic acid oxidation is shown in Fig 4.14a and 4.14b. Addition of CAF and its derivatives to the reaction decreased conjugated diene formation with dose-response relationship. The IC_{50} values of inhibition of AAPH- induced linoleic acid oxidation were calculated from the linear range. The IC_{50} values of CAF and its derivatives are shown in Table 4.1. The order of potency considering from the IC50 values was EDP> ODP>PEDPA≈EDPA≈PMDP>ODPA>CAF>PEDPA>PEDP. CAF derivatives, except PEDPA and PEDP, showed significantly higher in potency for 2-7 folds when compared with CAF. EDP had the highest potency among the test compounds. PEDP possessed the lowest inhibitory activity due to low stability of the compound.

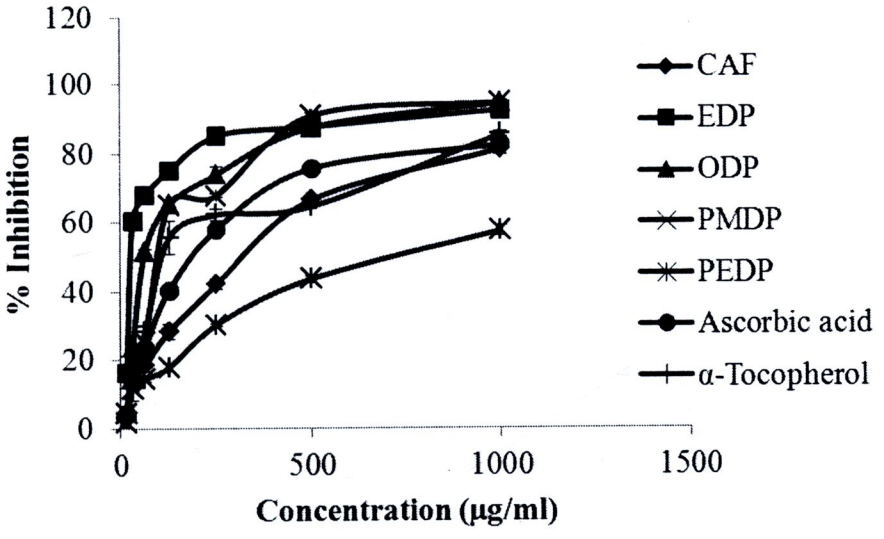

Fig 4.15a Percent inhibition of CAF and its ester derivatives on AAPH induced linoleic peroxidation

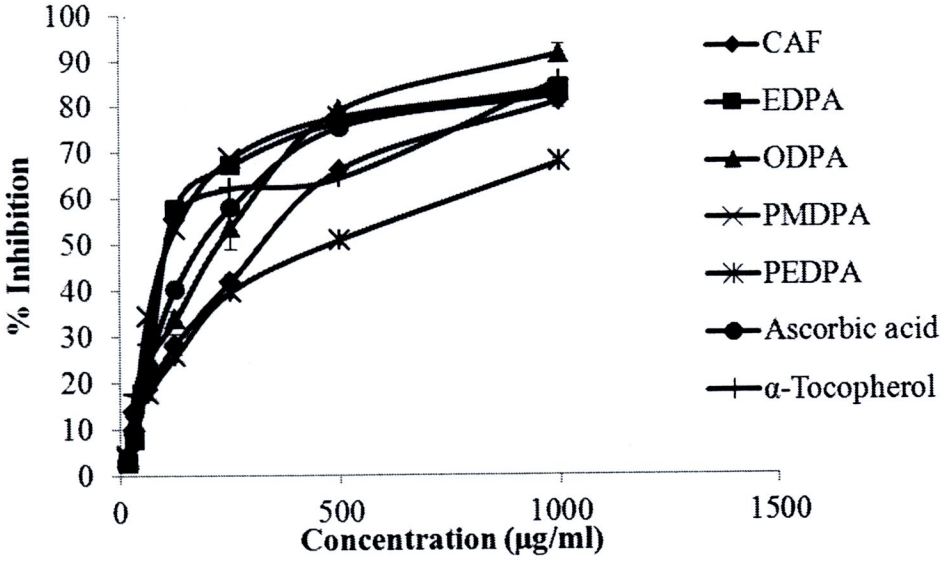

Fig 4.15b Percent inhibition of CAF and its amide derivatives on AAPH-induced linoleic peroxidation.

Table 4.1 The IC_{50} values of CAF and its derivatives on free radical scavenging

Tested substances	IC_{50} values (μg/ ml) analysed by different methods				
	DPPH	Deoxyribose assay	PMS-NADPH-NBT system	Sodium nitroprusside	linoleic acid oxidation
CAF	74.49	4.13×10^{-3}	36.47	19.15	173.15
EDP	70.00	4.16×10^{-3}	157.74	24.16	46.99
ODP	184.56	4.21×10^{-3}	103.71	37.34	60.37
PMDP	285.34	4.26×10^{-3}	113.10	52.64	116.82
PEDP	866.54	4.02×10^{-3}	112.99	>1,000	495.83
EDPA	61.32	4.17×10^{-3}	44.56	45.77	116.68
ODPA	245.11	4.31×10^{-3}	728.27	148.97	116.82
PMDPA	241.62	4.27×10^{-3}	586.14	59.12	116.48
PEDPA	878.12	4.39×10^{-3}	124.34	79.11	334.18
Ascorbic acid	263.70	4.02×10^{-3}	26.06	14.16	-
α-Tocopherol	382.98	4.23×10^{-3}	45.17	66.66	-

4.3 Determination of cytochrome P450 catalytic activities

4.3.1. Assay of CYP1A2 activity

CAF and its amide derivatives are widely used as antioxidants. They have been reported to exert a variety of beneficial and harmful effects. The results of this study add the evidence of beneficial effects by demonstrating the ability of CAF and its derivatives on inhibition of procarcinogen activating enzyme, CYP1A2, activity in pooled human liver microsomes. The inhibition of CYP1A2 activity by CAF and its derivatives were determined using phenacetin as a substrate. The amount of reaction product, acetaminophen, was measured as the area under the curve by using HPLC. CAF and its derivatives significantly inhibited the phenacetin *O*-deethylation reaction in a concentration-dependent manner. Mean IC_{50} values of CAF, and its derivatives are shown in Table 4.2.

According to characterization of the inhibition kinetic of CYP1A2, which was obtained from Cornish-Bowden (Fig.4.16) and Dixon plots (Fig.4.17), all plots indicated that CAF and its amide derivatives inhibited phenacetin *O*-deethylation by uncompetitive inhibition, whereas ester derivatives inhibited the reaction by mixed inhibition. Among all compounds tested, PEDPA has the lowest IC_{50} values (0.89 μM) indicating the most potent inhibitor of CYP1A2.

The modulation of CYP1A2 would be important from a clinical point of view, as this enzyme can activate or inactivate xenobiotics, including therapeutic agents [87]. Ryu and Chung, [88] showed that the long term consumption of the dietary supplement, ginkgo biloba can induce CYP1A2 activity which may increase the incidence of colorectal cancer. Previous studies have shown that hydrocinnamic

acids, such as chlorogenic acid, caffeic acid and ferrulic acid inhibited CYP1A2 – mediated methoxyresorufin *O*-demethylation in hamster liver microsomes [89].

This study demonstrated that CAF and its derivatives significantly inhibited CYP1A2 enzyme in human liver microsomes. The type of inhibition of CAF and its amide derivatives on CYP1A2 activity were uncompetitive inhibition. This suggested that CAF and its amide derivatives bound with enzyme- substrate complexes and became more potent as the substrate concentration rose. Moreover, the inhibition of CYP1A2 by CAF and its amide derivatives was time- and concentration- dependent and required NADPH. For ester derivatives of CAF, the inhibition was mixed type. CYP1A2 enzyme is composed of hydrophobic and aromatic amino acids with polar amino acids for hydrogen bonding being present near the heme centre [90] and CYP activities are related to lipophilic substance [91]. It is possible that hydrogen bonding and lipophicity interaction contribute to the inhibitory activities. The substances which have an *ortho*-or *para*- hydroxyl group can potently inhibit CYP1A2 [92]. According to the values of IC_{50}, PEDPA seems to be a potent inhibitor of CYP1A2. Regarding chemical structure, another benzene ring and longer carbon side chain resulting in more lipophilicity may contribute to stronger inhibitory effect on CYP1A2 activity compared with CAF. Inhibition of CYP1A2 activity by CAF and its derivatives may reduce bioactivation of procarcinogenic substrates. Therefore, its modulation can dramatically decrease the compound's toxicity and carcinogenesis. Kuenzig et al., [93] showed that CAF and ferrulic acid could react with nitrite *in vitro* and block the elevation of serum *N*- nitrosodiumthymine levels in rats, which plays a role in the body's defense against carcinogenesis.

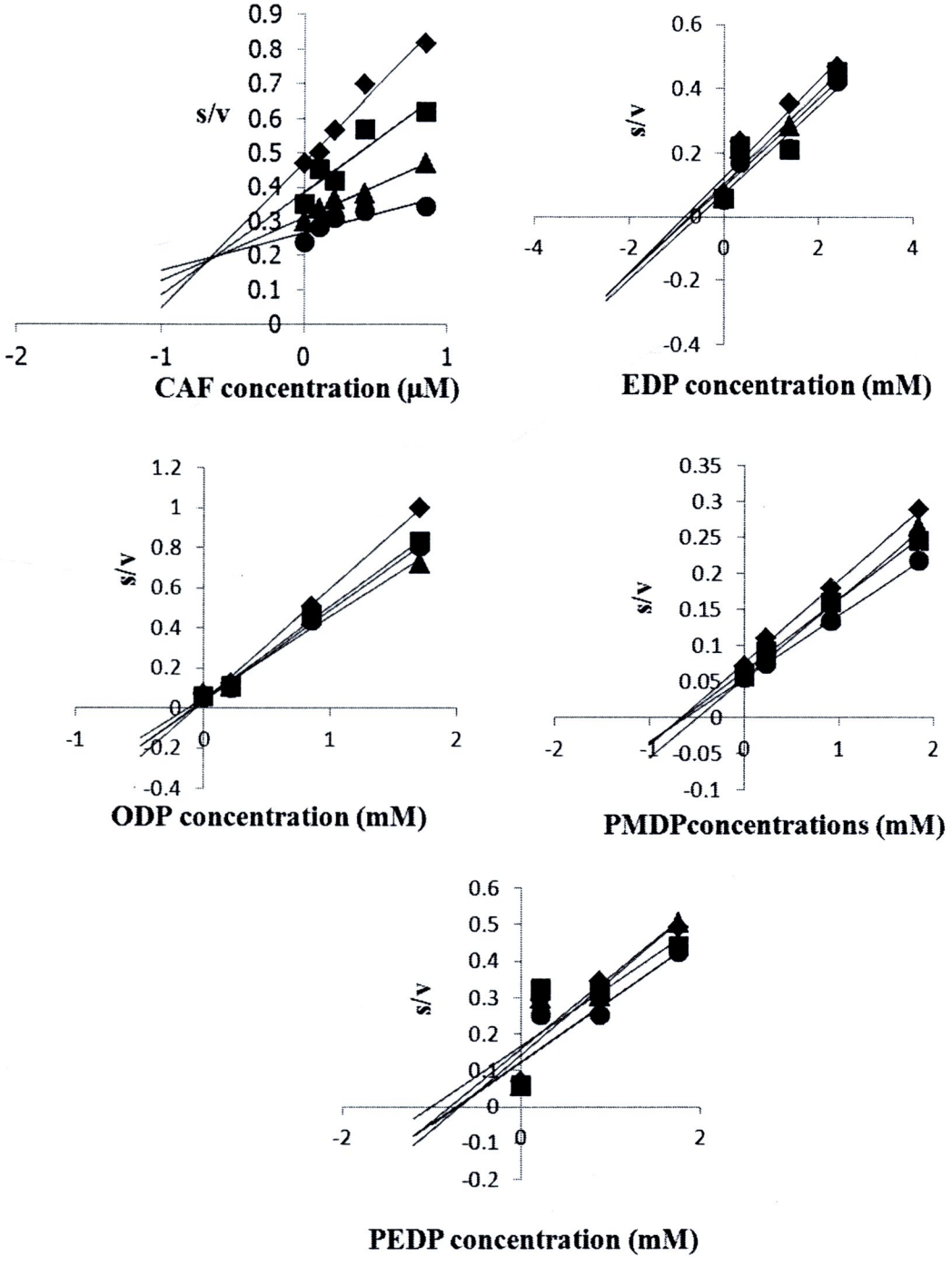

Fig. 4.16 Cornish-Bowden plot between s/v and caffeic acid ester derivatives concentrations (mM) of CYP1A2 activity. Values are average of triplicate determinations. ◆= 1.4 mM, ■= 0.84 mM, ▲=0.70 mM and ●= 0.50 mM of phenacetin concentrations.

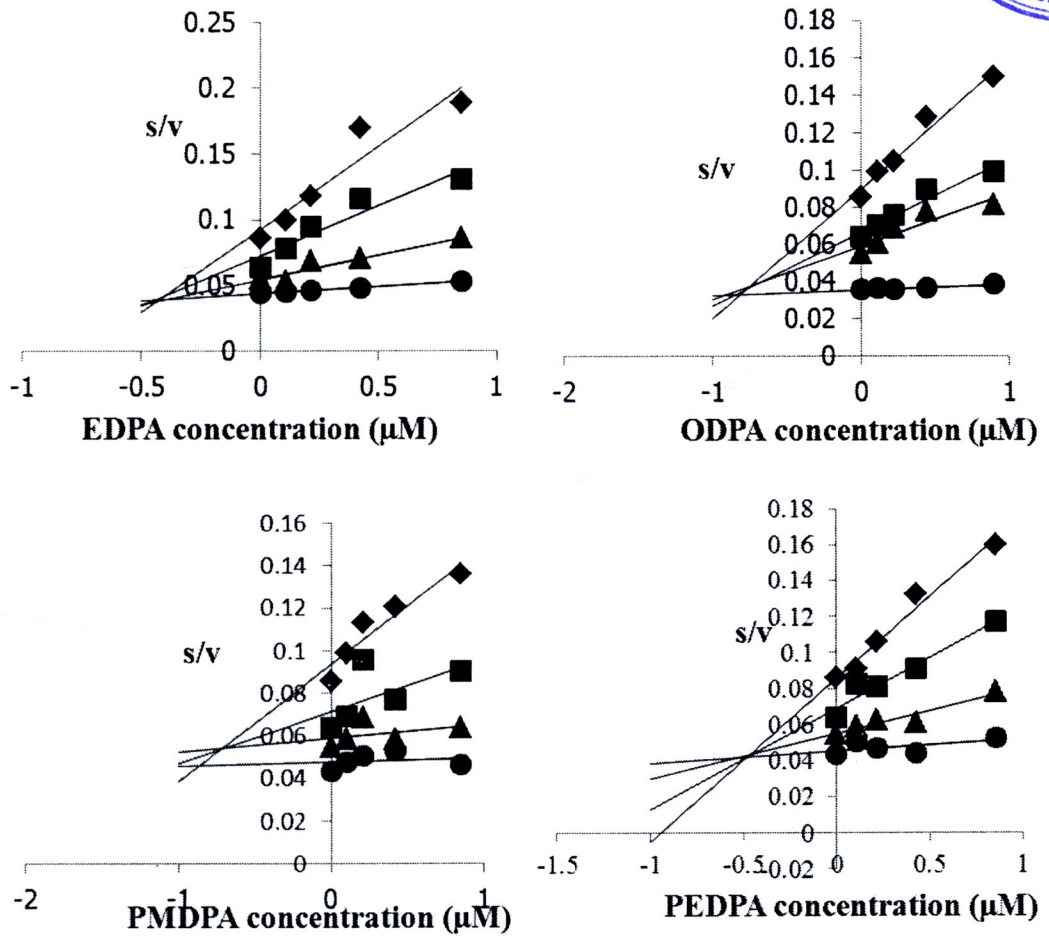

Fig. 4.16(con't) Cornish-Bowden plot between s/v and caffeic acid ester derivatives concentrations (mM) of CYP1A2 activity. Values are average of triplicate determinations. ◆= 1.4 mM, ■= 0.84 mM, ▲=0.70 mM and ●= 0.50 mM of phenacetin concentrations.

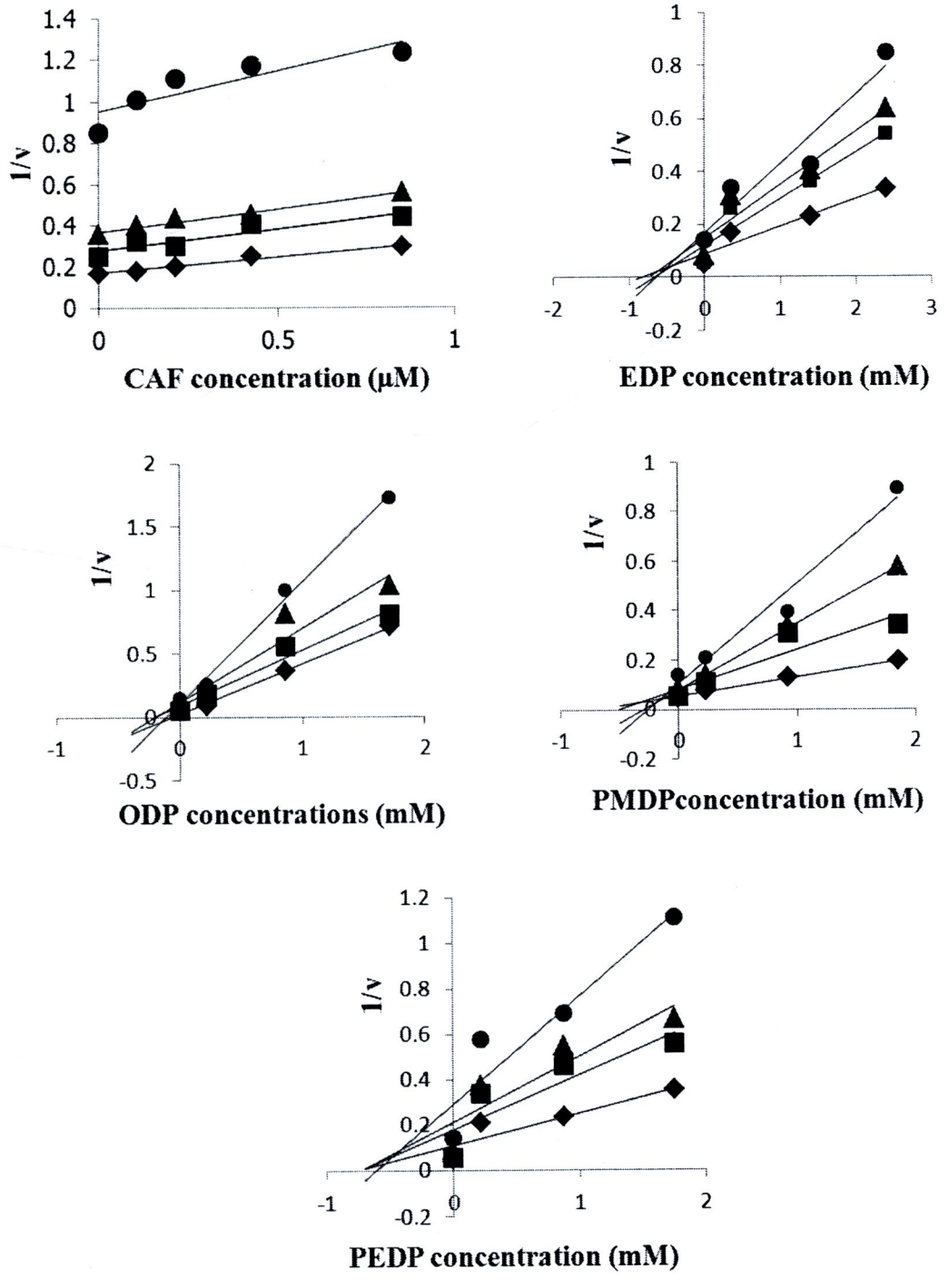

Fig.4.17 Dixon plot between 1/v and caffeic acid ester derivatives concentrations (mM) of CYP1A2 activity. Values are average of triplicate determinations. ◆= 1.4 mM, ■= 0.84 mM, ▲=0.70 mM and ●= 0.50 mM of phenacetin concentrations.

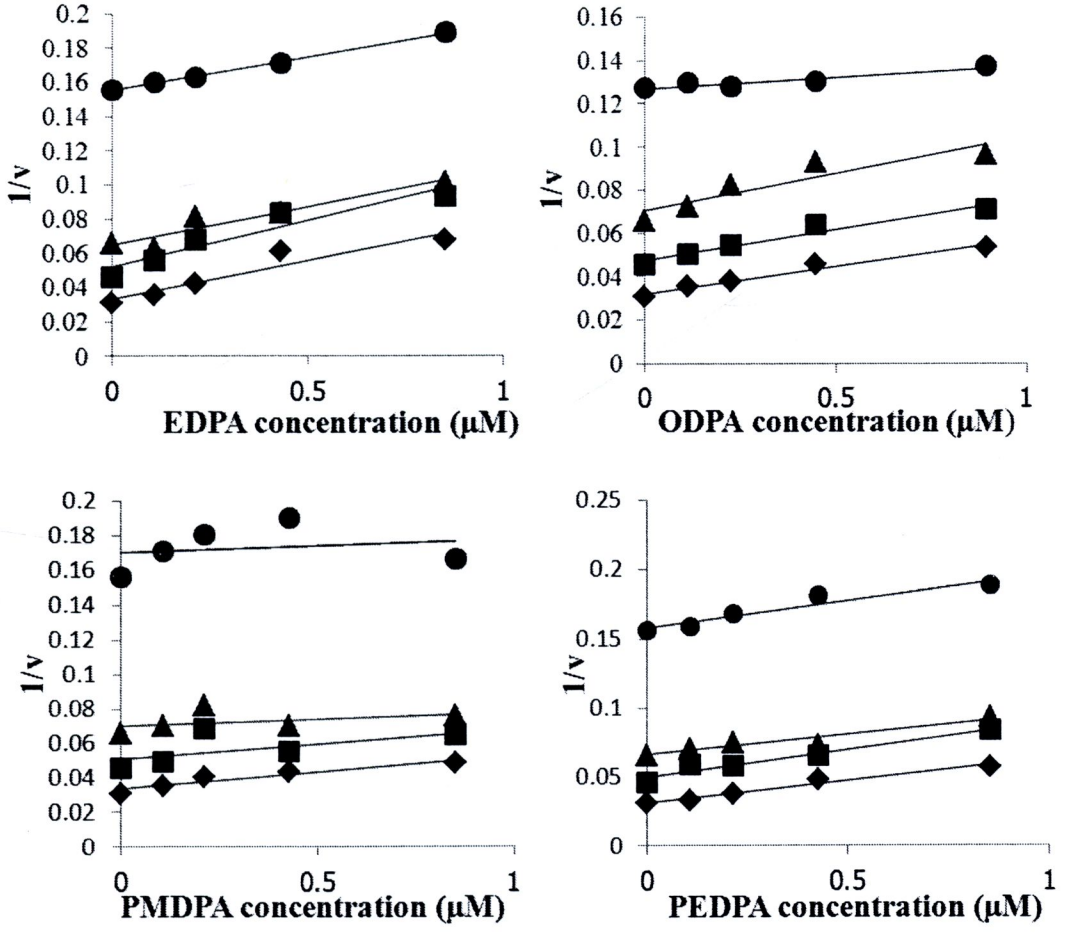

Fig.4.17 (con't) Dixon plot between 1/v and caffeic acid ester derivatives concentrations (mM) of CYP1A2 activity. Values are average of triplicate determinations. ◆= 1.4 mM, ■= 0.84 mM, ▲=0.70 mM and ●= 0.50 mM of phenacetin concentrations.

4.3.2. Assay of CYP2E1 activity

CYP2E1 has been implicated in the generation of ROS such as superoxide and hydrogen peroxide and may mediate the toxic effects of variety of xenobiotic compounds [94]. CYP2E1 has been distributed in many organs and involved in bioactivation process. Compounds which inhibit CYP2E1 activity may be useful in the prevention of chemical toxicity. There are many natural compounds that inhibit CYP2E1 activity. (-)- Epigallocatechin-3-gallate in tea was the most effective antimutagen and inhibits CYP2E1 [95]. Ellagic acid also inhibits CYP2E1 and reportedly reduces nitrosamine- induced tumors in rats [96]. A number of compounds have been suggested as metabolic markers of CYP2E1 activity including chlorzoxazone, ethoxycoumarin and *p*-nitrophenol. In this study, *p*- nitrophenol was selected as a probe to determine CYP2E1 activity. The amount of 4-nitrocatechol, the reaction product of *p*-nitrophenol hydroxylation was measured by using spectrophotometer. *p*-nitrophenol concentration in the reaction used less than 1.25 mM because the higher concentrations can be inhibited CYP2E1 activities. CAF and its derivatives significantly inhibited the *p*- nitrophenol hydroxylation. The IC_{50} values of CAF and its derivatives are shown in Table 4.2. The ODP was the most potent inhibitor of CYP2E1 activity when comparing with CAF and other derivatives. The CAF derivatives, except ODP and EDP, were about two times greater in potency compared to CAF. The IC_{50} value of ODP was 14.4 folds less than that of CAF. CAF derivatives, except EC, strongly inhibited *p*-nitrophenol hydroxylation with concentration-dependent manner. Characterization of kinetic inhibition of CYP2E1 was evaluated from Cornish-Bowden and Dixon plots. According to Cornish-

Bowden plots (Fig.4.17) and Dixon plots (Fig. 4.18), CAF and its ester and amide derivatives showed uncompetitive inhibition on CYP2E1- mediated *p*-nirophenol hydroxylation. The general structural requirement for CYP2E1 substrate may mainly due to lipophilic character. The CAF composes carboxylic group and hydroxyl groups which possess hydrophilic property than its derivatives. Therefore, IC_{50} value of CAF was found to be the highest indicating low inhibitory effect on CYP2E1 activity. Bell-Parikh and Guengerich [97] reported that *in vitro* measurements of CYP2E1 metabolism of many substrates may be complicated by the existence of a rate-determining step between product formation and release. The results indicate that inhibition on CYP2E1 activity might lead to reduction of ROS and risk of carcinogenesis.

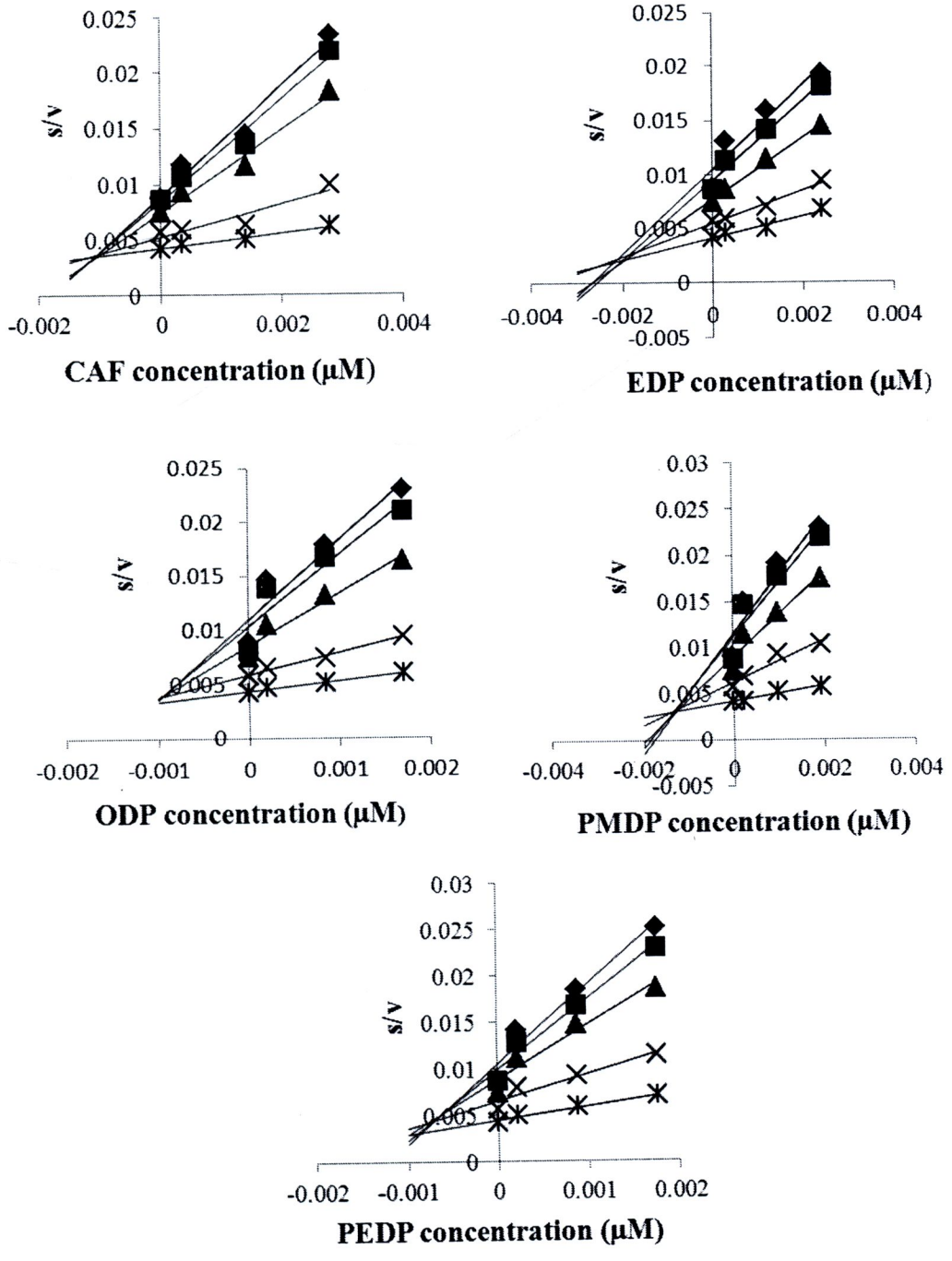

Fig.4.18 Cornish-Bowden plot between s/v and caffeic acid ester derivatives concentrations (mM) of CYP2E1 activity. Values are average of triplicate determinations. ◆= 1.2 mM, ■= 1.0 mM, ▲=0.6 mM , ×= 0.50 and ✳=0.15 mM of *p*-nitrophenol.

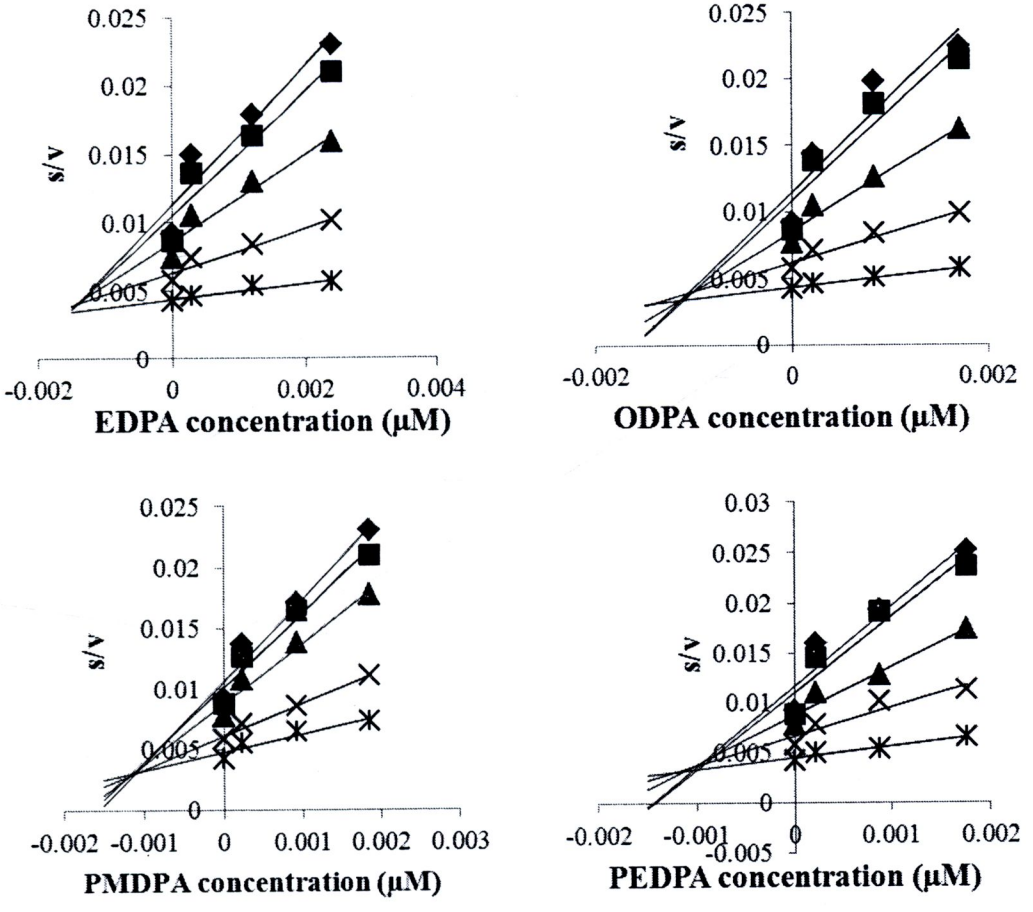

Fig.4.18 (con't) Cornish-Bowden plot between s/v and caffeic acid ester derivatives concentrations (mM) of CYP2E1 activity. Values are average of triplicate determinations. ◆= 1.2 mM, ■= 1.0 mM, ▲=0.6 mM , ×= 0.50 and ∗=0.15 mM of *p*-nitrophenol.

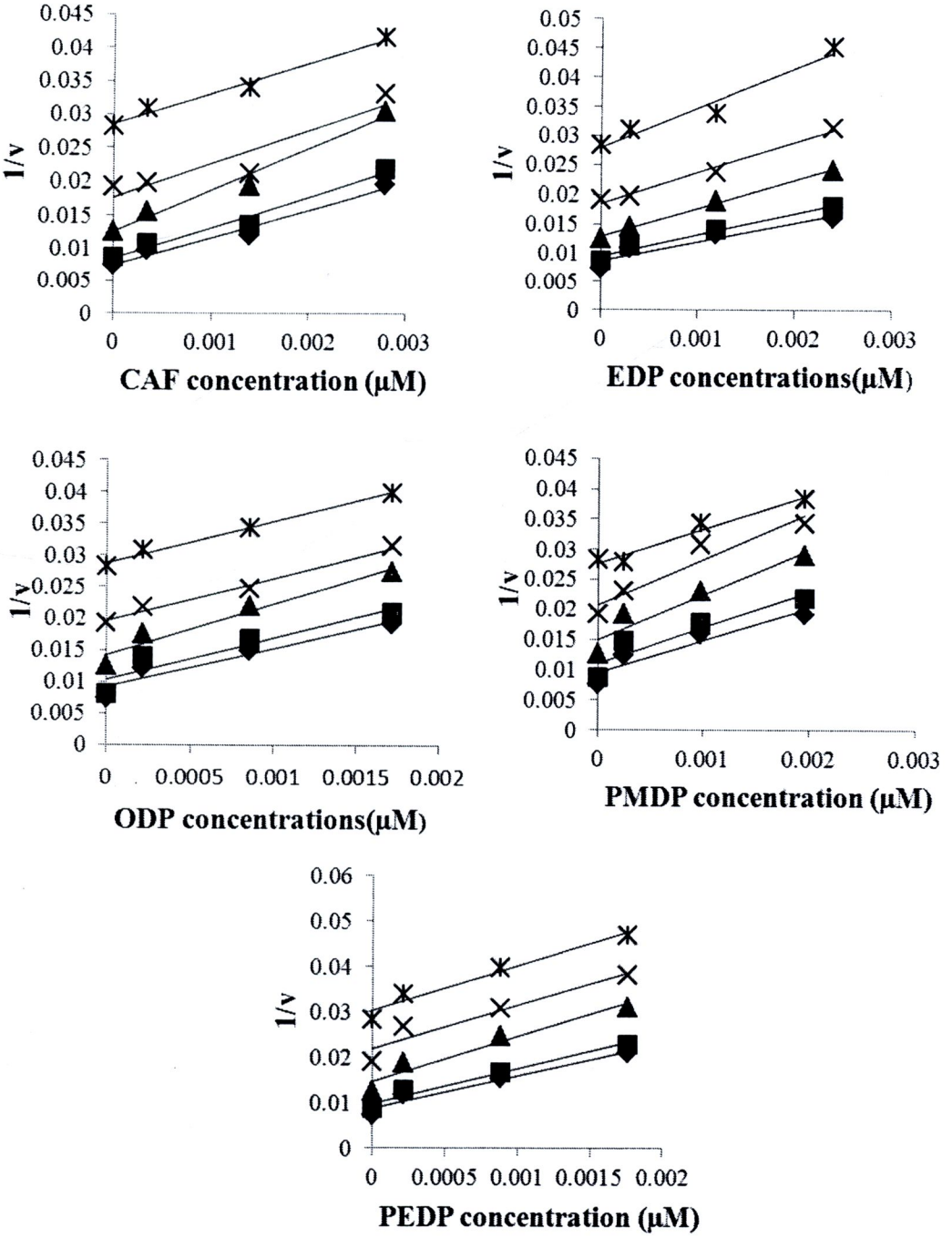

Fig.4.19 Dixon plot between 1/v and caffeic acid ester derivatives concentrations (mM) of CYP2E1 activity. Values are average of triplicate determinations. ◆= 1.2 mM, ■= 1.0 mM, ▲=0.6 mM , ×= 0.50 and ∗=0.15 mM of *p*-nitrophenol.

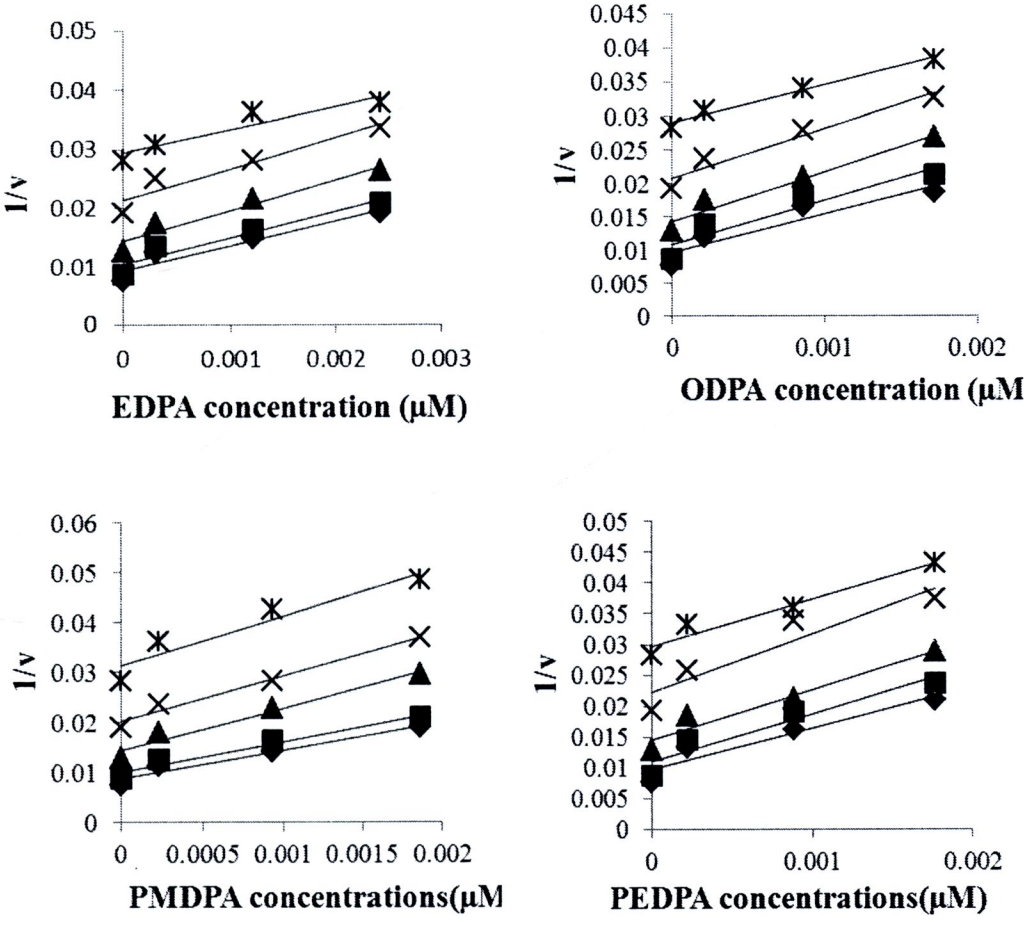

Fig.4.19(con't) Dixon plot between 1/v and caffeic acid ester derivatives concentrations (mM). Values are average of triplicate determinations. ◆= 1.2 mM, ■= 1.0 mM, ▲=0.6 mM , ×= 0.50 and ∗=0.15 mM of *p*-nitrophenol.

4.3.3. Assay of CYP3A4 activity

The CYP3A4 is the major enzyme in CYP3A family found in human liver and small intestine and estimate 50% contribution in metabolism of drugs in clinical use including acetaminophen, diazepam, erythromycin, codeine, cyclosporine A, midazolam, rifampicin and quinidine [98]. Kilicarslan *et al.* [99] indicated that diazepam is metabolized to oxazepam by CYP3A4 enzyme. In this study, we used diazepam as a probe and quantify amount of oxazepam to determine CYP3A4 activity.

The percent inhibition of CYP3A4 activity in human liver microsome using diazepam at concentration of 2.1 μM and the concentration of CAF and its derivatives at 0.0625 μg/ mL is showed that EDPA exhibited strong inhibition of 53.31± 2.46% on CYP3A4 activity when compared with control. The inhibitory effect of PMDPA, EDP, ODPA, PEDPA, CAF, PEDP, PMDP and ODP on CYP3A4 activity were 45.51±5.60, 43.63±2.37, 42.01±3.06, and 40.61±4.37, 34.70±2.68, 30.54±2.38, 27.70±3.39 and 22.63±1.95 % respectively. The IC_{50} values of CAF and derivatives are shown in Table 4.2. CAF and its derivatives inhibited CYP3A4 activities in a concentration-dependent manner, with IC_{50} values ranging from 0.31-0.82 μM, indicating that they are strong inhibitors against diazepam metabolism. The CAF analogues showed comparable inhibition on CYP3A4 activity. Moreover, amide analogues showed higher potential to inhibit diazepam metabolism than ester analogues with the same side chains for 1.1-2.6 folds. It is possible that the high polarity of substrates containing hydroxyl groups may contribute to inhibitory effect

on CYP3A4 activity enzyme [100]. In addition, Bu [101] reported that lipophilicity property decreased CYP3A4 activity.

The Ki values were calculated from linear regression. The Ki values of CAF, PMDPA, EC, PC, ODPA, PEDPA, EDPA, OC and BC were 0.24, 0.29, 0.49, 0.56, 0.57, 0.59, 0.62, 0.62 and 1.03 μM, respectively. According to characterization of the inhibition kinetic of CYP3A4 obtained from Cornish-Bowden plots (Fig. 4.20) and Dixon plots (Fig 4.21). CAF inhibited CYP3A4 by uncompetitive inhibition while ester and amide analogues showed competitive inhibition.

Normally, active site of CYP3A4 appears capable of accommodating a wide range of structure from simple to macromolecules. It showed that CYP3A4 enzyme tends to oxidize lipophilic substances or basic compounds [102]. This is consistent with previous observation with CYP3A4 pharmacophore models and the apparent lack of functionality in the amino acid residues comprising the CYP3A4 active site which composing of leucine 210, leucine 211 and aspartic acid 214 [103]. *N*-containing heterocyclic in the structure appeared to increase the potential of CYP3A4 inhibition. Then CAF amide derivatives were more potent to inhibit CYP3A4 than ester derivatives. It seems that this reflects increased binding energy afforded by the lone pair electron on nitrogen atom ligating to the CYP heme iron about 6 kcal/ mol as suggested for the prototypic CYP inhibitor including ketoconazole, sulfaphenazole, carbamazepine, quinidine, verapamil [104] and grapefruit juice [105]. Grapefruit juice composed of CAF, coumaric acid, sinapic acid and ferrulic acid [106]. Identification of the herbs bioactive compounds will help to understand the mechanism and can avoid side effects of herbs-drug interaction.

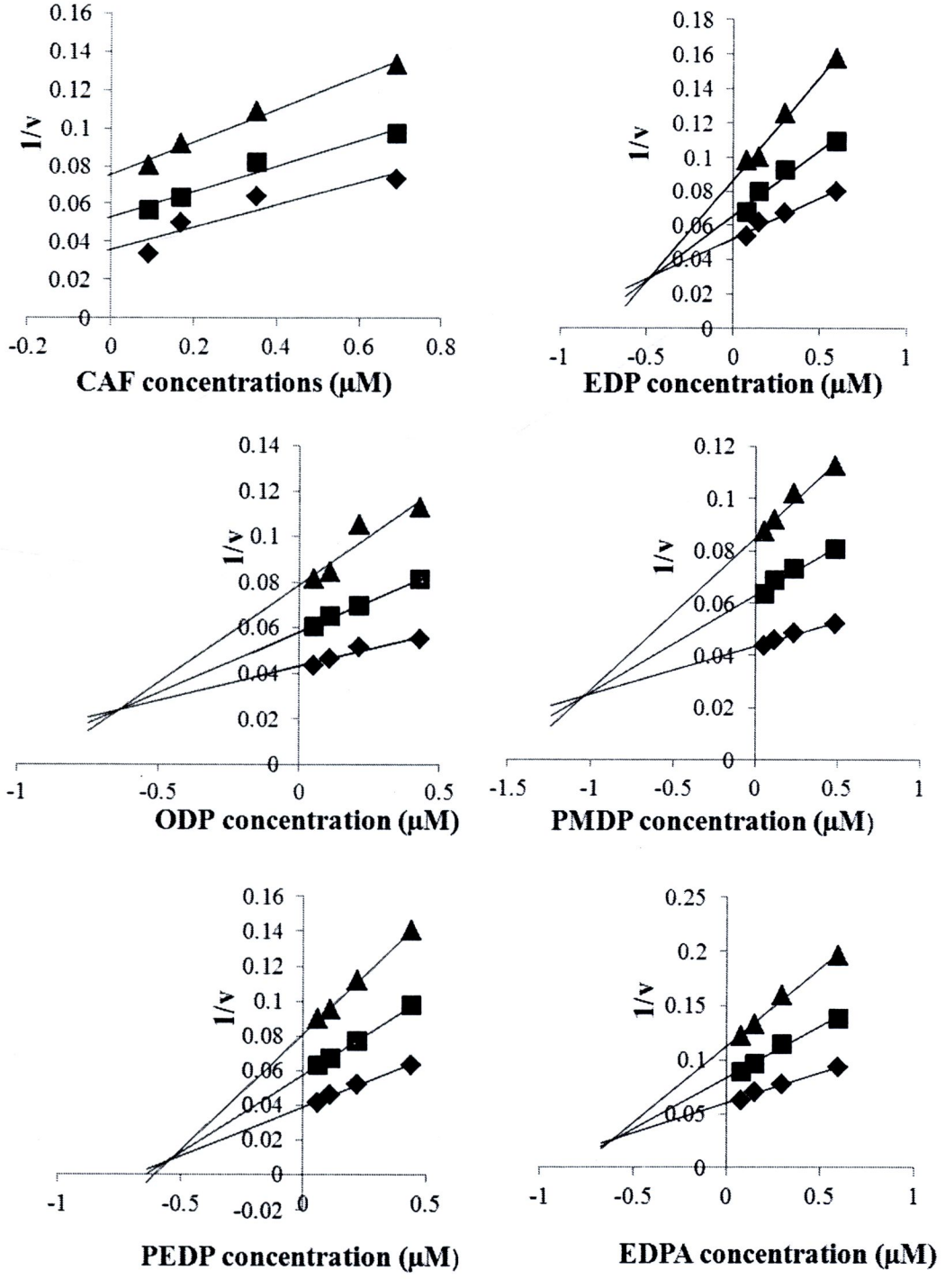

Fig.4.20 Cornish-Bowden plot between s/v and caffeic acid ester derivatives concentrations (mM) of CYP3A4 activity. Values are average of triplicate determinations. ▲ 1.39, ■ 2.08, ◆ 3.47 μM of diazepam.

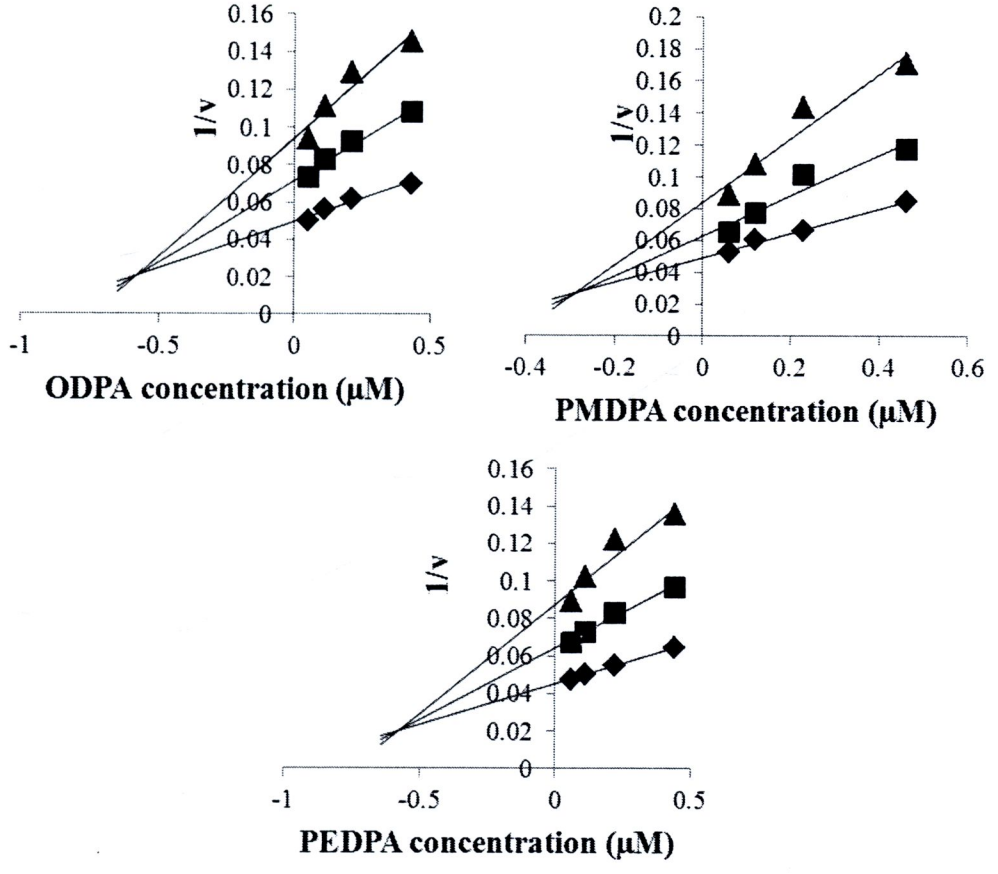

Fig.4.20 (con't) Cornish-Bowden plot between s/v and caffeic acid ester derivatives concentrations (mM) of CYP3A4 activity. Values are average of triplicate determinations. ▲ 1.39, ■ 2.08, ◆ 3.47 μM of diazepam.

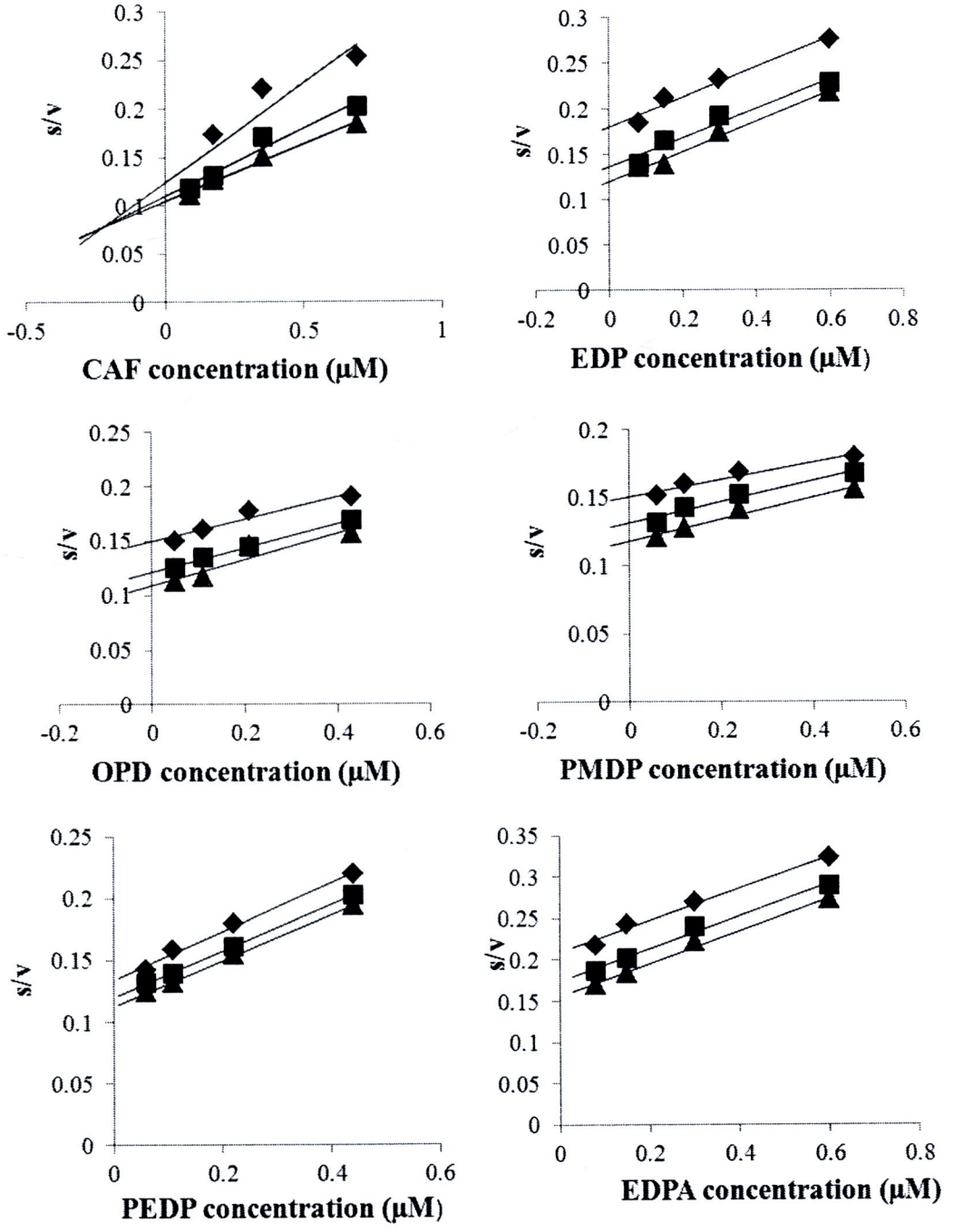

Fig.4.21 Dixon plot between 1/v and caffeic acid ester derivatives concentrations (mM) of CYP3A4 activity. Values are average of triplicate determinations. ▲ 1.39, ■ 2.08, ◆ 3.47 μM of diazepam.

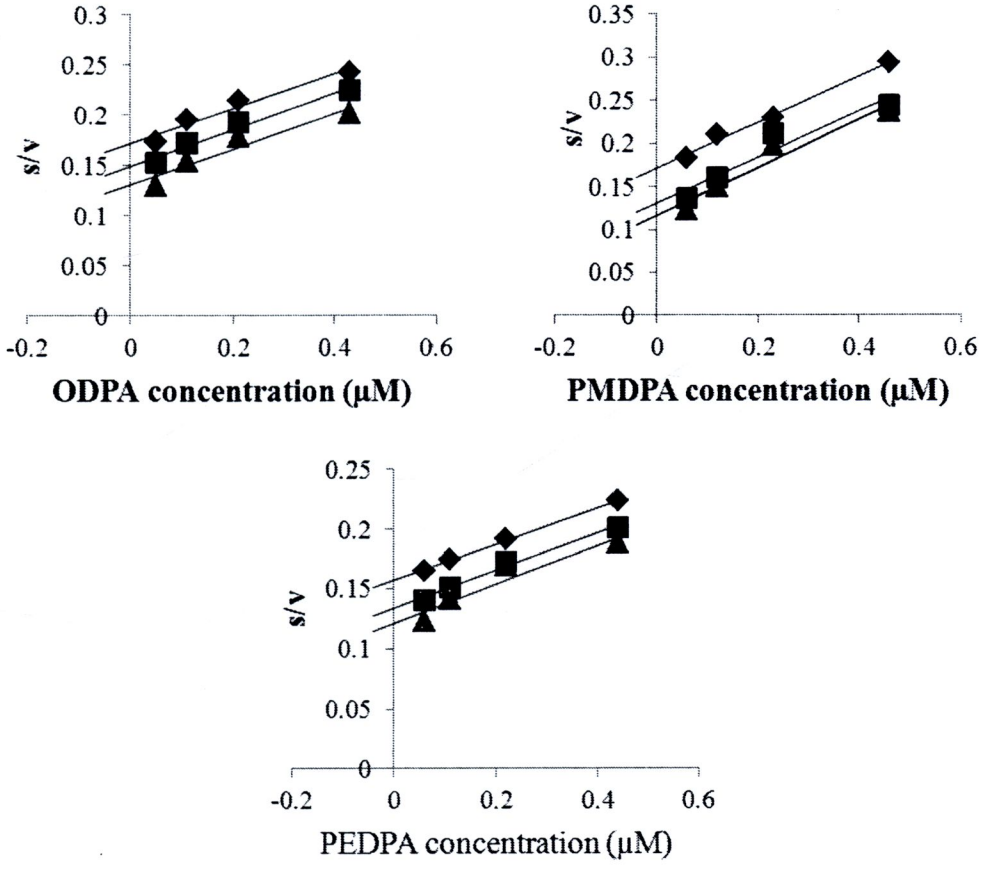

Fig.4.21 (con't) Dixon plot between 1/v and caffeic acid ester derivatives concentrations (mM) of CYP3A4 activity. Values are average of triplicate determinations. ▲ 1.39, ■ 2.08, ◆ 3.47 μM of diazepam

Table 4.2 The IC_{50} values of CAF and its derivatives on microsomal enzyme systems

Tested substances	IC_{50} (μM) on different microsomal enzyme systems		
	CYP1A2	CYP2E1	CYP3A4
CAF	1.57	2.02	0.31
EDP	124.98	1.92	0.37
ODP	111.86	0.14	0.46
PMDP	156.68	0.99	0.49
PEDP	31.05	0.87	0.53
EDPA	0.39	1.21	0.58
ODPA	0.80	0.84	0.72
PMDPA	0.75	1.11	0.75
PEDPA	0.45	0.62	0.82

4.4. Phase 2 enzyme assays

4.4.1. UDP-glucuronosyl transferase

In mammalia animals, glucuronidation is a major conjugation reaction involved in metabolic elimination of exogenous and endogenous compounds. This reaction is catalyzed by UDP- glucuronosyltransferase (UGT) which is typical membrane protein of endoplasmic reticurum and nuclear envelop. The expression of several UGT isoform in mammals is reported influently by inducers belonging to different substances for example, polyaromatic hydrocarbons, phenobabital, clofibrate, glucocorticoid and antioxidants. Interestingly, UGT inducers have been found in food such as oltipraze in cruciferous vegetables and phenethyl isothiocyanate in watergrass. Flavonoid, chrysin can induce UGT1A1 mRNA and protein in Caco-2 and Hep G2 cells. In this experiment, human hepatoma cell line Hep G2 was used to examine induction of glucuronidation activity by CAF and its derivatives. Hep G2 microsomal UGT activities were compared with the control group by using *p*-nitrophenol as a substrate [107].

Fig. 4.22 shows effects of CAF on UGT activity in Hep G2 cell line. Five concentrations of CAF including 41.67, 83.33, 161.11, 194.44 and 388.89 μM were used in this study. After the cells were treated for 12 h, UGT activity was decresed in the higher doeses. After treating with 194.44 and 388.89 μM of CAF for 24 to 72 h, the UGT activities were higher when compared with the control group ($p<0.05$).

Hep G2 cells were treated with 9.62, 19.23, 37.98, 48.08 and 72.12 μM of EDP, the result is shown in Fig. 4.23. At 6 and 12 h, the UGT activity was not changed, except at the highest dose, 72.12 μM, that the activity was decreased. The

UGT were activated after treating the Hep G2 cells with 9.62, 19.23 μM of EDP for 24 to 72 h. The highest UGT activity value was 1.38 mmol PNP conjugated / min/ mg protein.

The Hep G2 cells were determined for UGT activities after treatment with 8.56, 17.12, 32.53, 51.37, 68.49 μM of ODP for 6 to 72 h. The result is shown in Fig. 4.24. The UGT activities were diminished after treating the cells with higher doses of ODP. The maximum of UGT activity was 0.71 mmol PNP conjugated/ min/ mg protein.

Fig. 4.25 shows the effects of PMPD on the UGT activity . Various concentrations of PMPD (2.93, 5.86, 12.11, 19.53, 23.44 μM) were used to treat Hep G2 cells for 6 to 72 h. After treatment for 6, 12 and 24 h, UGT activity was decreased when compared with the control group. The maximun UGT activity were 0.73 mmol PNP conjugated/ min/ mg protein at 48 h after treating with 19.53 μM of PMDP.

35.21, 70.42, 99.30, 140.85 and 211.27 μM of PEDP were treated on Hep G2 cells for measuring UGT activity. The effects of PEDP on UGT activity is shown in Fig. 4.26. The UGT activities were decreased after treating with high concentration for 6 and 12 hours. UGT activities were similar to those of control groups when Hep G2 cells were treated longer than 12 h.

Fig. 4.27 shows the effects of EDPA on UGT activity. When the cells were treated with 1.21, 2.42, 5.31, 9.66 and 19.32 μM of EDPA for 72 hour, the UGT activities were higher than those of control group ($p<0.05$). At 6, 12 and 24 hours the UGT activities were not changed compared with those of control groups except the

cells treated with the highest concentration (19.32 μM) that UGT activity was decreased.

Fig 4.28 shows the effect of ODPA on UGT activity after treating the Hep G2 cells with 5.15, 10.31, 21.65, 51.55 and 103.09 μM of ODPA. At 6 h, ODPA did not have any effect on the UGT activity. Meanwhile,UGT activities of the cells treated with high concentration of ODPA for 12 and 24 h were significantly decreased compared with those of control groups ($p<0.05$). The ODPA activated the UGT activities after treating the cells for 48 and 72 hours.

Hep G2 cells were treated with 0.93, 1.86, 3.35, 7.43, and 14.87 μM of PMDPA for 6 to 72 hours. Fig 4.29 shows the effects of PMDPA on UGT activity. The results show that the UGT activity was induced after treating with PMDPA for 72 hours. At 6 to 48 hour after treatment UGT activity was not significantly induced or inhibited.

Fig 4.30 shows the effect of PEDPA which was 1.77, 3.53, 4.59, 7.07 and 14.13 μM on the UGT activity. The results show that PEDPA had no effect on UGT activity, except 0.5 μM of PEDPA which was significantly increased UGT activity when compared with the control group.

In this study, curcumin and β-napthoflavone were used as positive controls. Fig 4.31 shows the effect of curcumin to induce UGT activity in Hep G2 cells. The result shows that curcumin induced maximum UGT activity after treating with 0.05 and 0.11 μM of curcumin for 24 hours. Treatment for longer than 24 h produced no significant different on UGT activity when compared with those of control groups. Fig 4.32 shows effect of β-napthoflavone on UGT activity after treating the cells were

treated with 25.71, 51.41, 102.83 and 205.66 μM. When the cells were treated with 51.41 μM of β-napthoflavone, the UGT activity was maximized with 0.7 p-nitrophenol-conjugated/ min/ mg protein. The results show that CAF and EDP were highly potent to induce UGT activity and the suitable times to determine UGT were 24 and 48 hours. The results of this study demonstrated that UGT activity toward *p*-nitrophenol (UGT1A6) increased in the Hep G2 cell. UGT1A6 is important in the detoxification of aromatic compounds, substrates for UGT1A6, including CAF and its derivatives which aromatic containing in the molecule. UGT proteins are membrane proteins with a hydrophobic membrane spanning domain at their carbonyl terminus in addition to other hydrophobic domain throughout the molecule, which probably function to bind hydrophobic molecules. After treatment the Hep G2 cells with CAF and derivatives for 6 to 12 hour, the results show the UGT activity were decreased. The evidence may suggest that glucuronic acid, cofactor of UGT enzyme, was used to bind with CAF and derivatives and excrete them out of the cell. Saracino and Lampe showed that phytochemicals such as phenolic acid and polyphenols could increase hepatic UGT activity. Phytochemicals concentration, duration of exposure, and/ or differences in model system may significantly affect on UGT activity and expression. Several ligand-activated transcription factors regulate phytochemical induction of UGTs, including the aryl hydrocarbon (AhR), pregnane and xenobiotic receptors (PXR), steroid and xenobiotic receptor (SXR) and nuclear factor erythroid 2- related factors (Nrf2) pathways [108]. The induction mechanism of UGT activity should be study in the future.

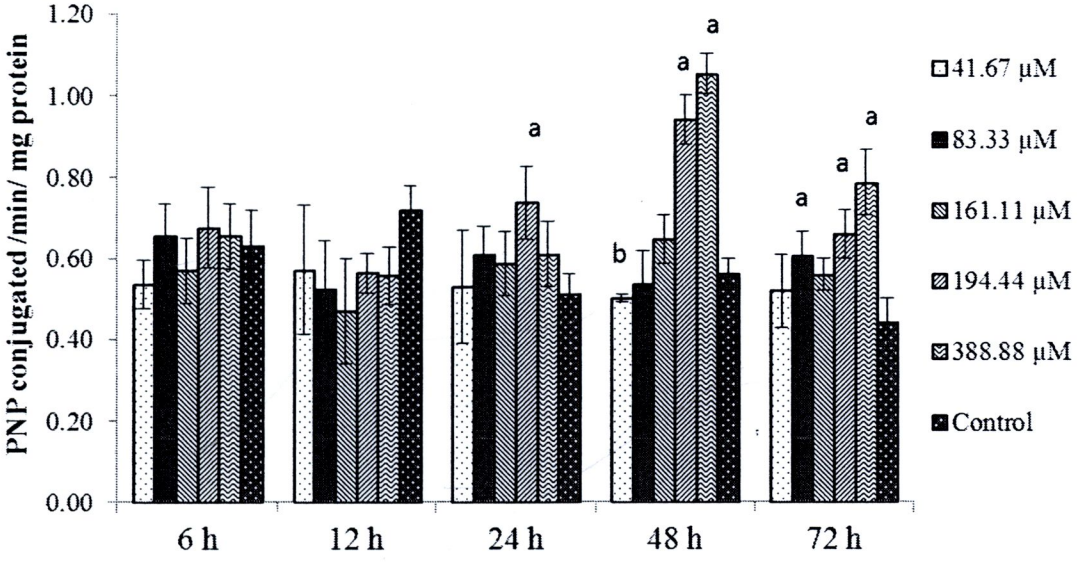

Fig. 4.22. UGT activity of Hep G2 cells treated with CAF for 6, 12, 24, 48 and 72 h.

a significantly higher than the control group of each time ($p < 0.05$)

b significantly lower than the control group of each time ($p < 0.05$)

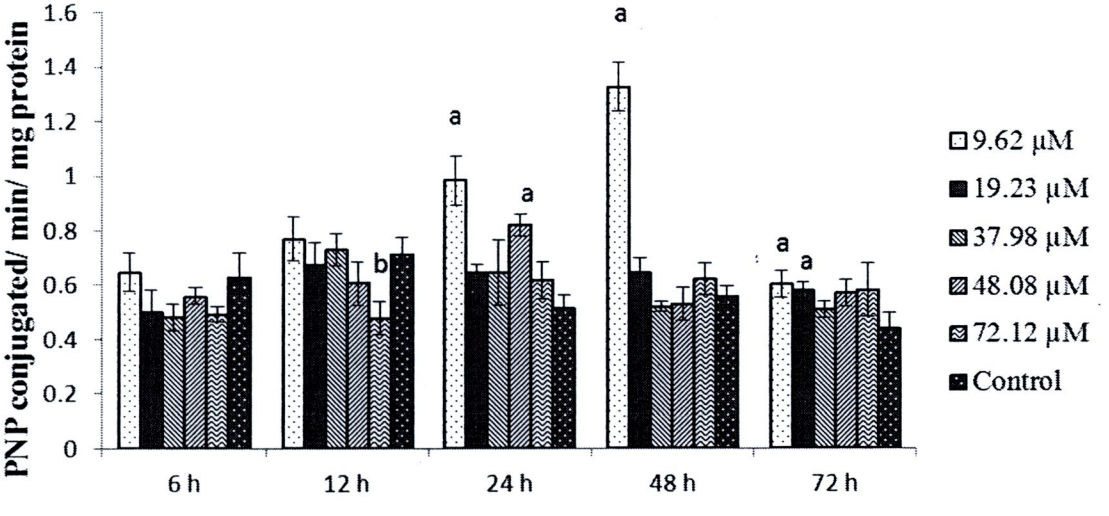

Fig. 4.23. UGT activity of Hep G2 cells treated with EDP for 6, 12, 24, 48 and 72 h.

a significantly higher than the control group of each time ($p < 0.05$)

b significantly lower than the control group of each time ($p < 0.05$)

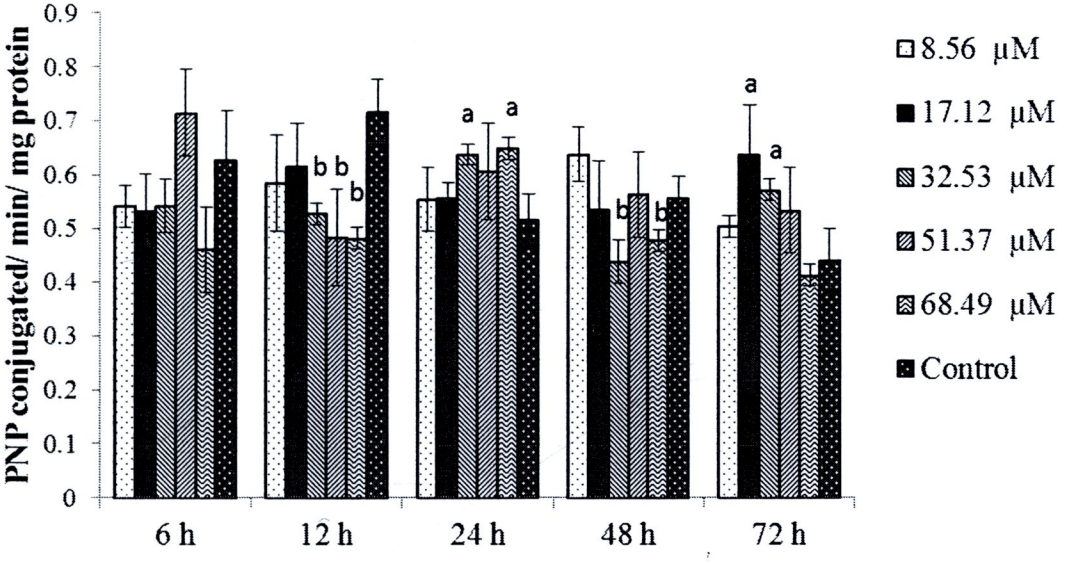

Fig. 4.24. UGT activity of Hep G2 cells treated with ODP for 6, 12, 24, 48 and 72 h.

a significantly higher than the control group of each time ($p < 0.05$)

b significantly lower than the control group of each time ($p<0.05$)

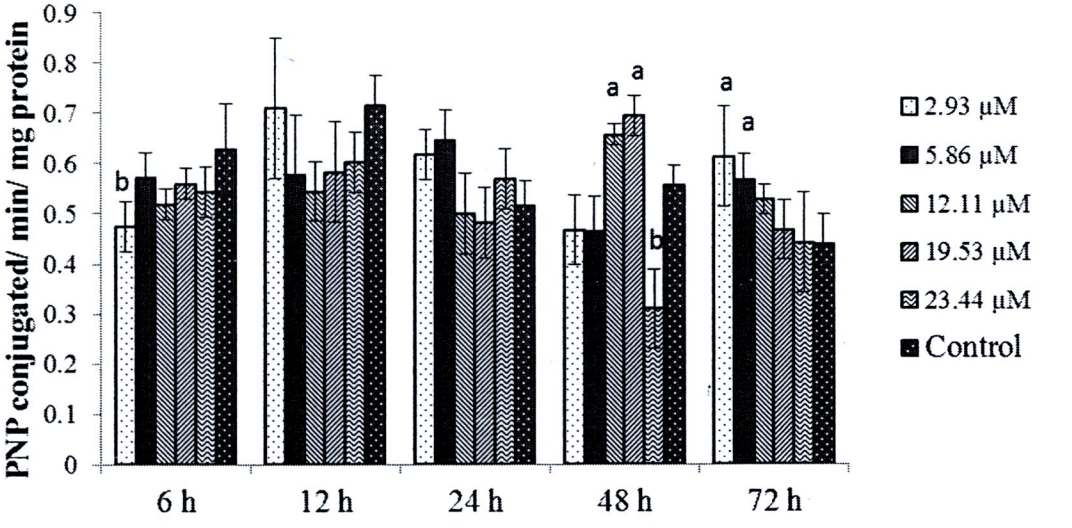

Fig. 4.25 UGT activity of Hep G2 cells treated with PMDP for 6, 12, 24, 48 and 72 h

a significantly higher than the control group of each time ($p < 0.05$)

b significantly lower than the control group of each time ($p<0.05$)

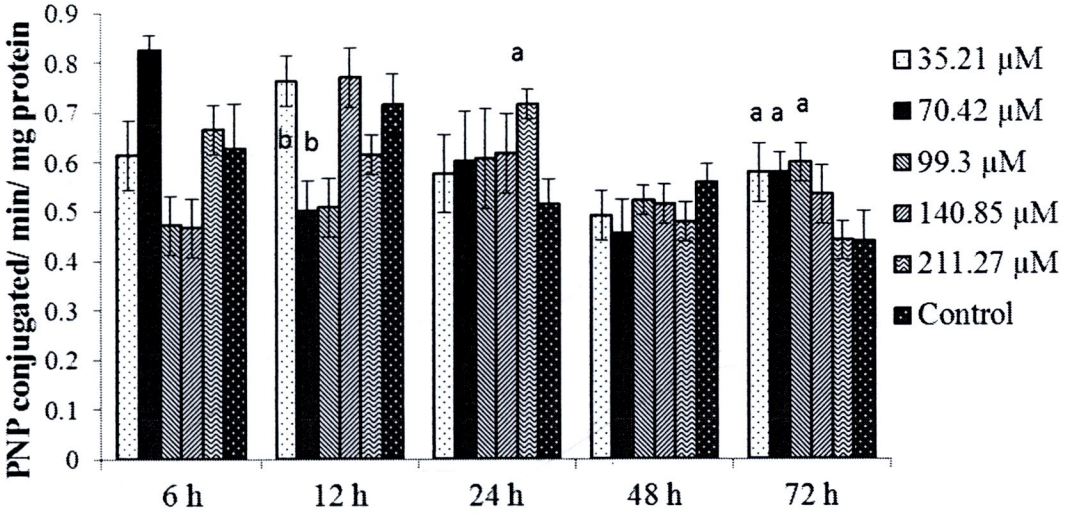

Fig. 4.26. UGT activity of Hep G2 cells treated with PEDP for 6, 12, 24, 48 and 72 h

a significantly higher than the control group of each time ($p < 0.05$)

b significantly lower than the control group of each time ($p < 0.05$)

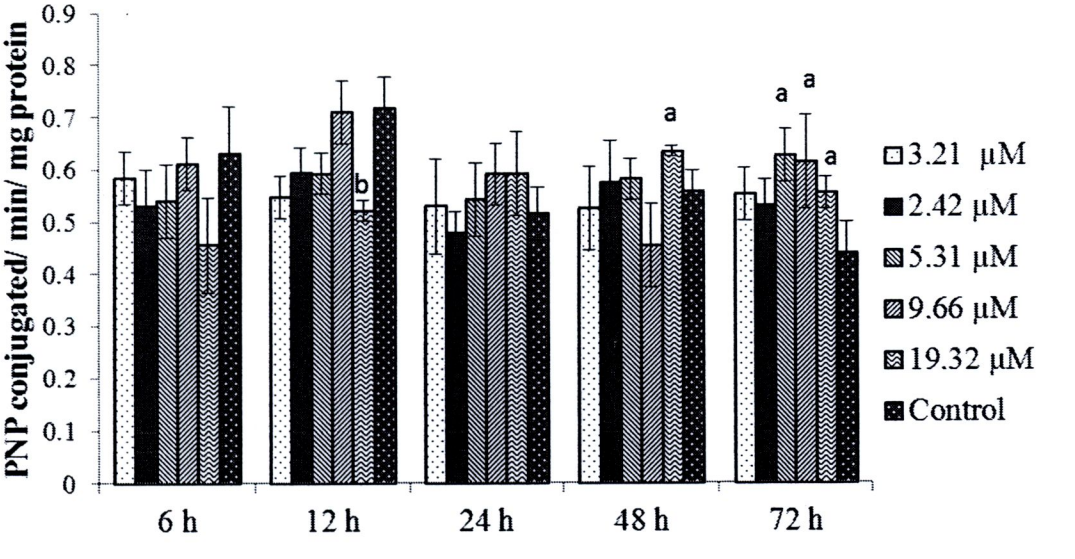

Fig. 4.27. UGT activity of Hep G2 cells treated with EDPA for 6, 12, 24, 48 and 72 h

a significantly higher than the control group of each time ($p < 0.05$)

b significantly lower than the control group of each time ($p < 0.05$)

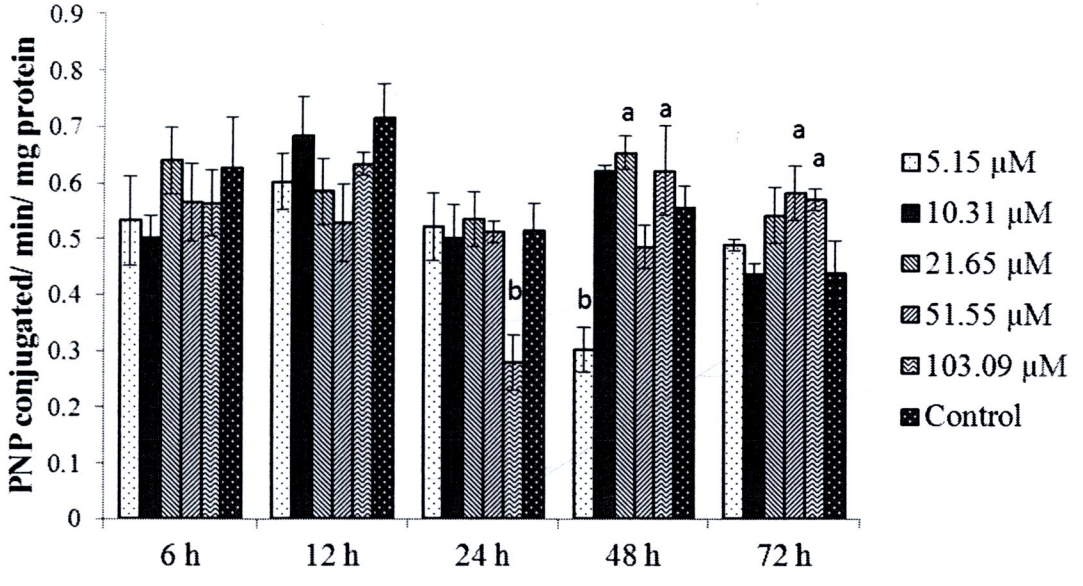

Fig. 4.28. UGT activity of Hep G2 cells treated with ODPA for 6, 12, 24, 48 and 72 h

a significantly higher than the control group of each time ($p < 0.05$)

b significantly lower than the control group of each time ($p<0.05$)

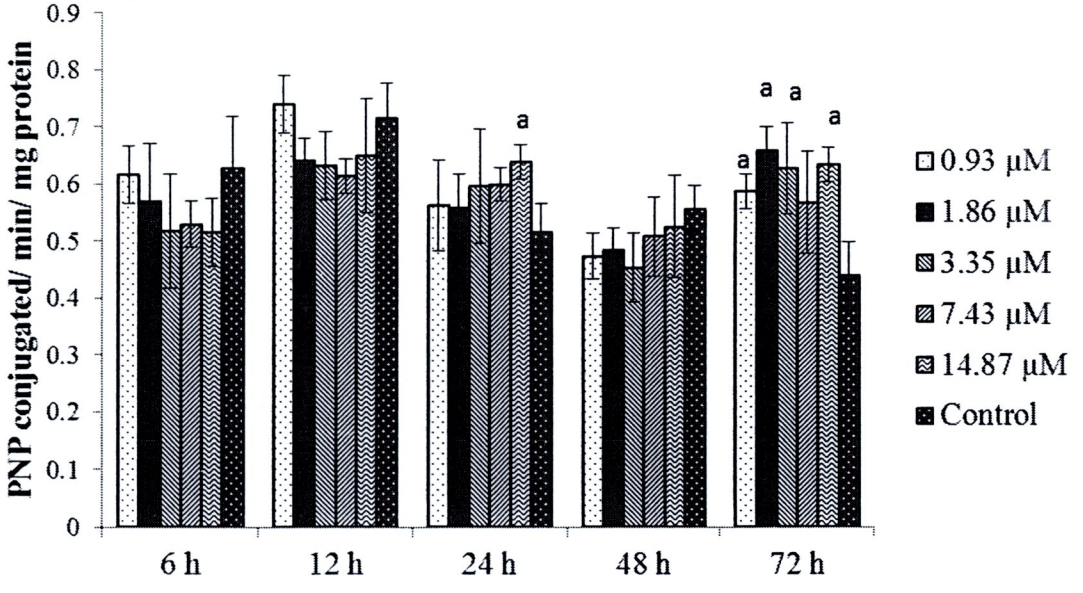

Fig. 4.29 UGT activity of Hep G2 cells treated with PMDPA for 6, 12, 24, 48 and72 h

a significantly higher than the control group of each time ($p < 0.05$)

b significantly lower than the control group of each time ($p<0.05$)

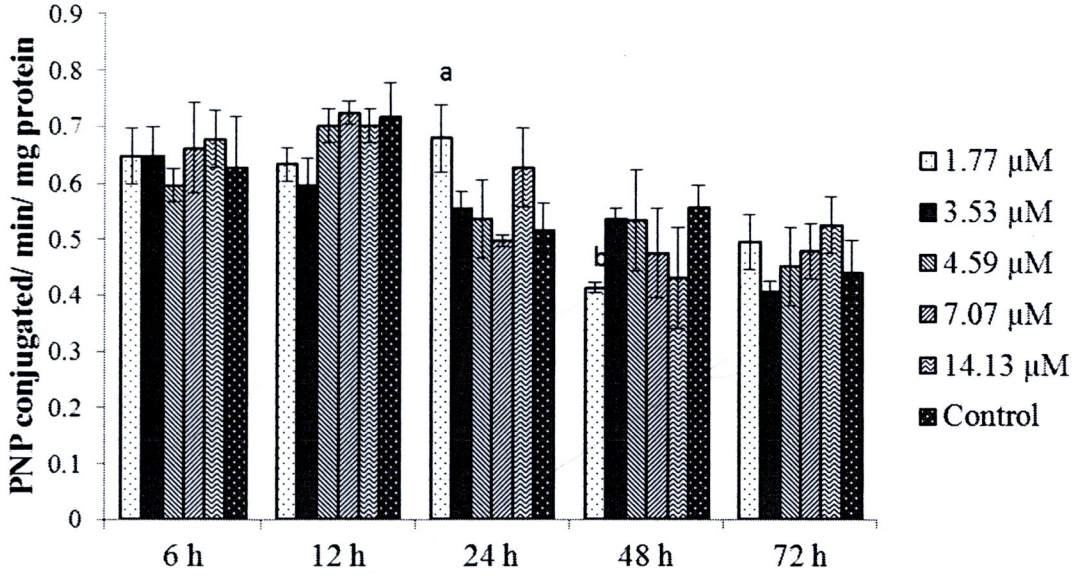

Fig. 4.30.UGT activity of Hep G2 cells treated with PEDPA for 6, 12, 24, 48 and72 h. *a* significantly higher than the control group of each time ($p < 0.05$) *b* significantly lower than the control group of each time ($p<0.05$)

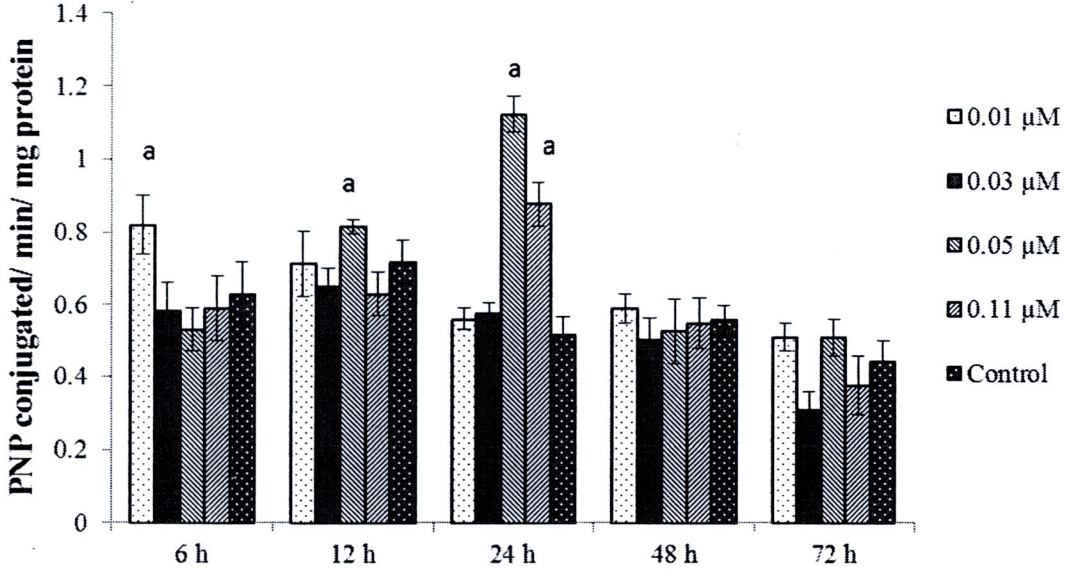

Fig. 4.31. UGT activity of Hep G2 cells treated with curcumin for 6, 12, 24, 48 and 72 h. *a* significantly higher than the control group of each time ($p < 0.05$), *b* significantly lower than the control group of each time ($p<0.05$)

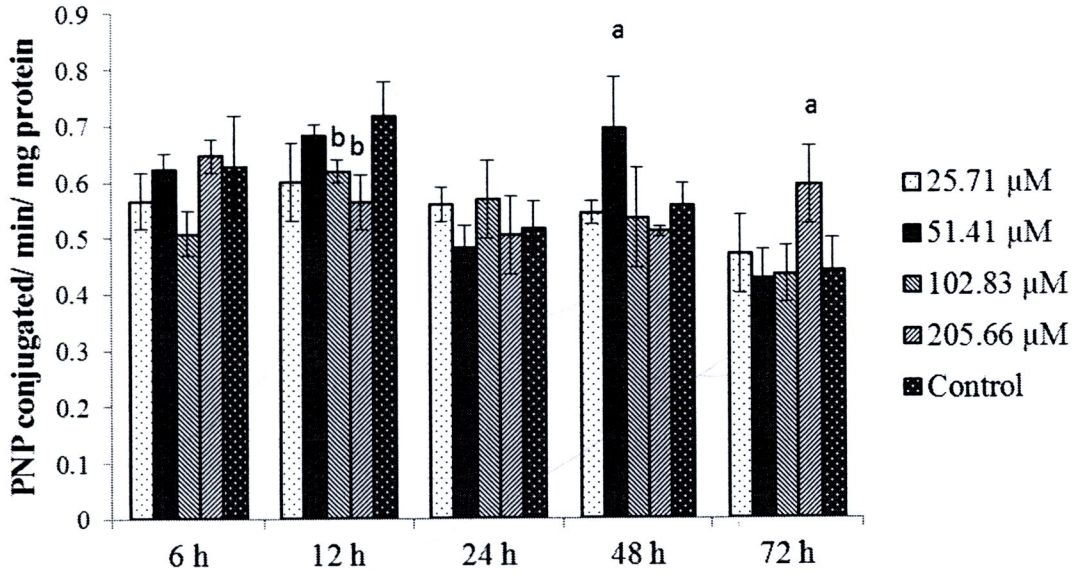

Fig. 4.32 UGT activity of Hep G2 cells treated with β- napthoflavone for 6, 12, 24, 48 and 72 h. *a* significantly higher than the control group of each time ($p < 0.05$), *b* significantly lower than the control group of each time ($p<0.05$)

4.4.2. Glutathione S transferase

After CAF and its derivatives were added in various concentrations and incubation for 6-72 hour and then Hep G2 cells were lysed. The levels of GST activity were measured using CDNB as substrate. CDNB used for measuring total GST activity composed GST alpha, mu, omega, pi, theta and zeta isoform [109]. The amount of GST in these base line cells was 0.3 Units/ mg protein which compared to previous reports on this cell line 0.090±0.011 U/mg protein [110], 0.014 U/ mg protein [111], 0.045±0.0028[112] and 0.112±0.004 U/ mg protein [113]. The results show that GST activity of the cells after incubating with the CAF and its derivatives for 6-48 hr decreased when compared with the control group.

GST activity was measured after treating with various concentration of CAF. The result is shown in Fig 4.33. After treatment the HepG2 cells for 6 and 12 hour, the GST activities were decreased when compared with the control group ($p< 0.05$). GST activity of the cells treated with 161.11 and 388.89 μM increased at 48 and 72 hour, respectively.

Fig 4.34 shows the effect of EDP on GST activity. The GST activity of HepG2 cells treated with high concentration of EDP decreased when compared with those of control group at 6 and 12 hour. The GST activity increased when the cells were treated with 48.08 μM of EDP for 24 hour.

Hep G2 cells were treated with various concentration of ODP. The result is shown in Fig. 4.35. The GST activity of the cells received high concentration of ODP decreased after treating for 12 and 24 hour. At 48 and 72 hour, the GST activities were similar in all ODP concentration when compared with the control groups.

Fig 4.36 shows the effects of PMDP on GST activity. The GST activity decreased after treating with high concentrations for 6 and 72 hour. GST activity was maximum with 0.42 U/ mg protein after treating the cell with 19.53 μM of PMDP for 48 hour.

GST activity of Hep G2 cells after treating with PEDP is shown in Fig 4.37. At 6, 12 and 24 hour, the GST activity decreased especially when treated with 99.3 and 140.85 μM of PEDP ($p<0.05$). The GST activity was induced 0.41 U/ mg protein when compared with those of control group ($p<0.05$) after treatment with 140.85 μM of PEDP.

The GST activity was determined on Hep G2 cell with EDPA. The result is shown in Fig 4.38. At 6, 12 and 24 hour after treating with EDPA, the GST activities decreased except the cells treated with 2.42 μM of EDPA that GST activity was induced compared to those of control group. After treatment for 48 and 72 hour, the GST activities were higher than those of control groups especially the cells treated with 2.42 and 19.32 μM of EDPA, respectively.

Fig 4.39 shows the GST activity in Hep G2 cells treated with various concentrations of ODPA. High concentrations of ODPA, 103.09 μM, decreased the GST activity after treating the cells for 6, 12 and 24 hour. At 48 hour, the GST activity was induced especially the cells treated with 103.09 μM of ODPA when compared with those of control group ($p<0.05$). After treatment the cells for 72 hour, 51.55 μM of ODPA induced the GST activity which was 0.55 U/ mg protein.

Various PMDPA concentrations were treated on Hep G2 cells. After treatment the cells with 1.86 and 3.35 μM for 6 and 12 hour, the GST activity

decreased significantly when compared with the control groups. At 48 and 72 hour, the GST activity increased especially at dose of 14.87 μM which activity was 0.56 U/ mg protein. The result is shown in Fig. 4.40.

Fig. 4.41 shows the GST activity after treatment with PEDPA. At 6 hour, the GST activity decreased with 4.59, 7.07 and 14.13 μM of PEDPA. At 12 hour, GST activity was activated using 7.07 μM with 0.42 U/ mg protein. The enzyme activity at 24 and 48 hour were similar when compared with the control groups. Treatment with 14.13 μM of PEDPA for 72 hour, the GST activity was maximum with value of 0.43 U/ mg protein.

Curcumin was used as positive control of GST acitivty. The result presented in Fig. 4.42. Treatment of the cell with 0.05 μM of curcumin could activate the GST activity for 12 hour with value of 0.59 U/ mg protein. GST activity of Hep G2 cells treated with 0.01 μM of curcumin for 24 hour, increased. The GST activities at 48 and 72 hour after treatment were similar value when compared with the control groups.

β-napthoflavone, a positive control, could affect GST activity which the result shows in Fig. 4.43. 102.83 and 205.66 μM of β-napthoflavone were treated on Hep G2 cells for 6 and 12 hour and GST activities decreased significantly compared with those of control group. The cells were treated for 48 hour with 51.41 μM of β-napthoflavone, resulting in the maximum GST activity with value 0.41 U/ mg protein.

Amide derivatives significantly induced GST activity after treating the cells with EDPA, ODPA, PMDPA and PEDPA for 72 hours. Comparing between ester and amide derivatives, amide derivatives seem to induce GST activities better than

ester derivatives. CAF ester and amide derivatives are significantly induce GST activities better than curcumin and β-napthoflavone serve as positive controls. Conjugation of glutathione to a wide variety of electrophilic chemicals is a vital detoxification reaction such as xenobiotics and reactive metabolites. GSTs are involved in their conjugation reaction by catalyzing the neucleophilic attack of glutathione (GSH) on electrophilic moieties of substrates.

Many researches showed that phenolic acid from plants extract can inhibit GST activity in many cancer cells types. CAF and its derivatives are type of phenolic acid which the results show inhibition of GST activity after treatment the cells for 6 to 24 hours. Moridani and co-worker showed that metabolism pathway of CAF, chlorogenic and dihydrocaffeic acid via glutathione conjugate pathway. Evelo and co-worker [114] reported that GST is damaged possibly by oxidation of thiol group containing in active site. The decrease in available GST activity plus the fact the GST activity is GSH dependent might imply that *in vivo* functioning of the enzyme. CAF, dihydrocinnamic acid are metabolized by conjugating with GSH, this event resulting in reduction of GSH levels in the cells. This reason may describe why GST activity was decreased at 6 and 12 hour.

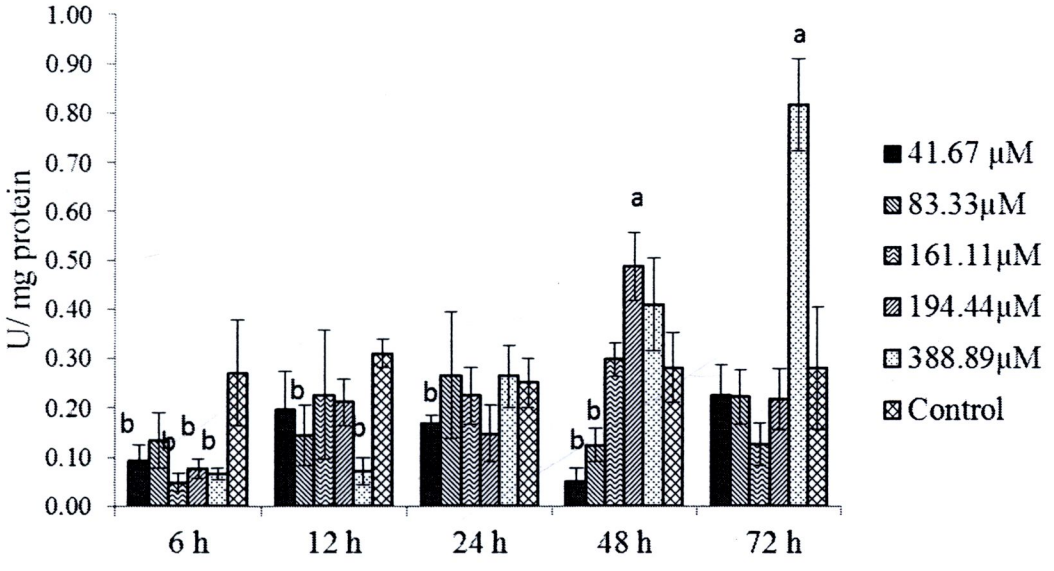

Fig. 4.33 GSTs activity in Hep G2 cells incubated for 6, 12, 24, 48 and 72 h with CAF. *a* significantly increased ($p < 0.05$) and *b* significantly decreased ($p<0.05$) when compared with the control group.

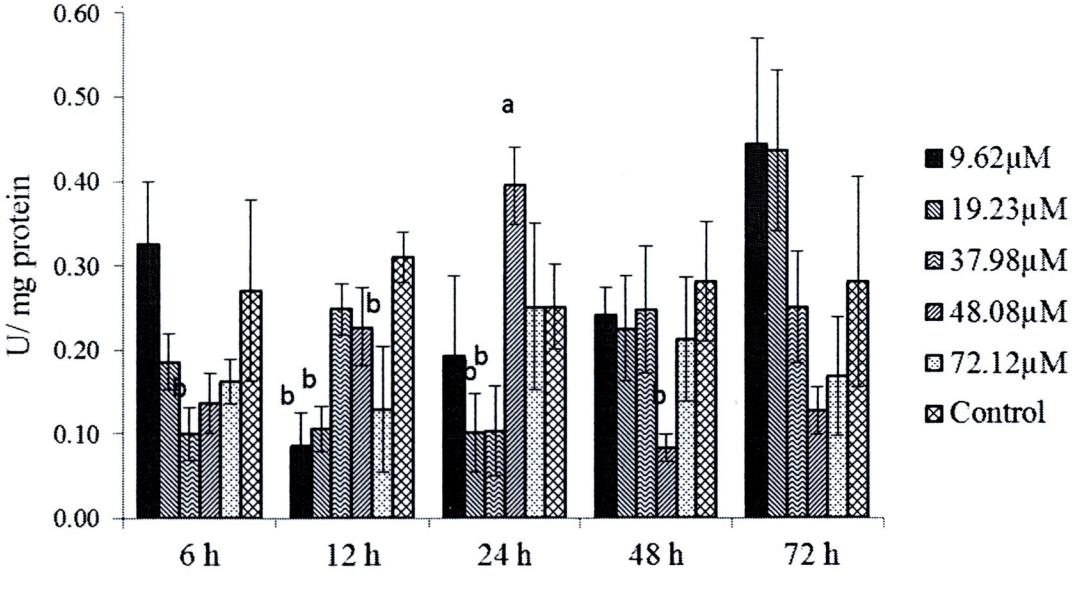

Fig. 4.34. GSTs activity in Hep G2 cells incubated for 6, 12, 24, 48 and 72 h with EDP. *a* significantly increased ($p < 0.05$), *b* significantly decreased ($p<0.05$) when compared with the control group.

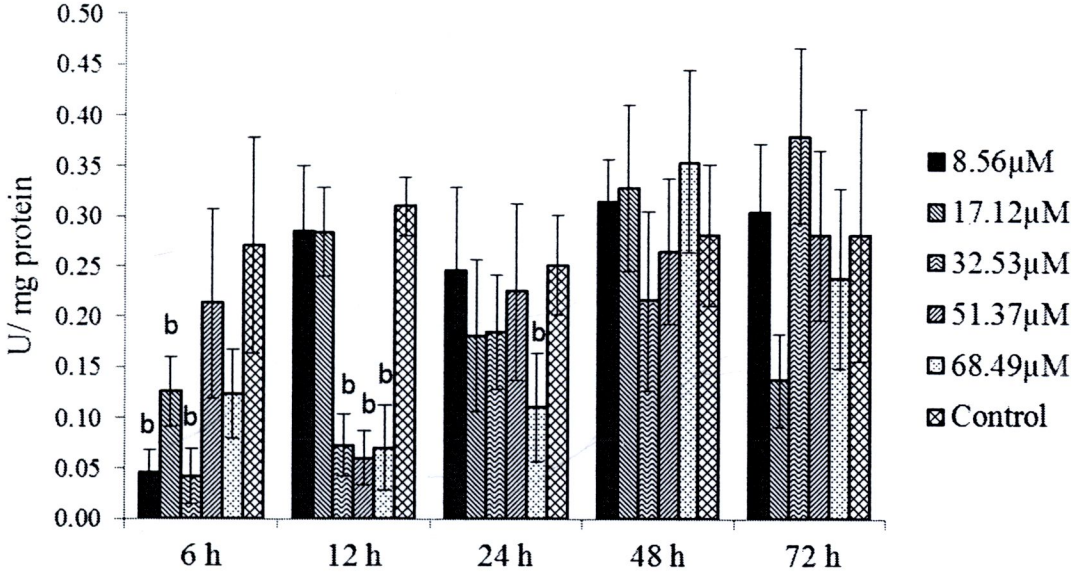

Fig. 4.35. GSTs activity in Hep G2 cells incubated for 6, 12, 24, 48 and 72 h with ODP. *a* significantly increased ($p < 0.05$) and *b* significantly decreased ($p<0.05$) when compared with the control group.

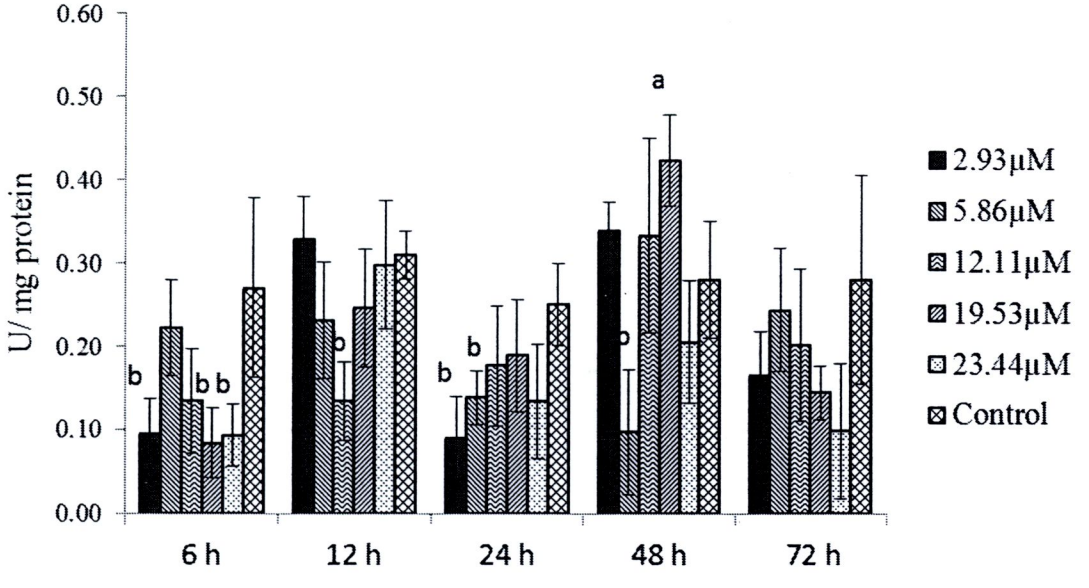

Fig. 4.36. GSTs activity in Hep G2 cells incubated for 6, 12, 24, 48 and 72 h with PMDP. *a* significantly increased ($p < 0.05$) and *b* significantly decreased ($p<0.05$) when compared with the control group.

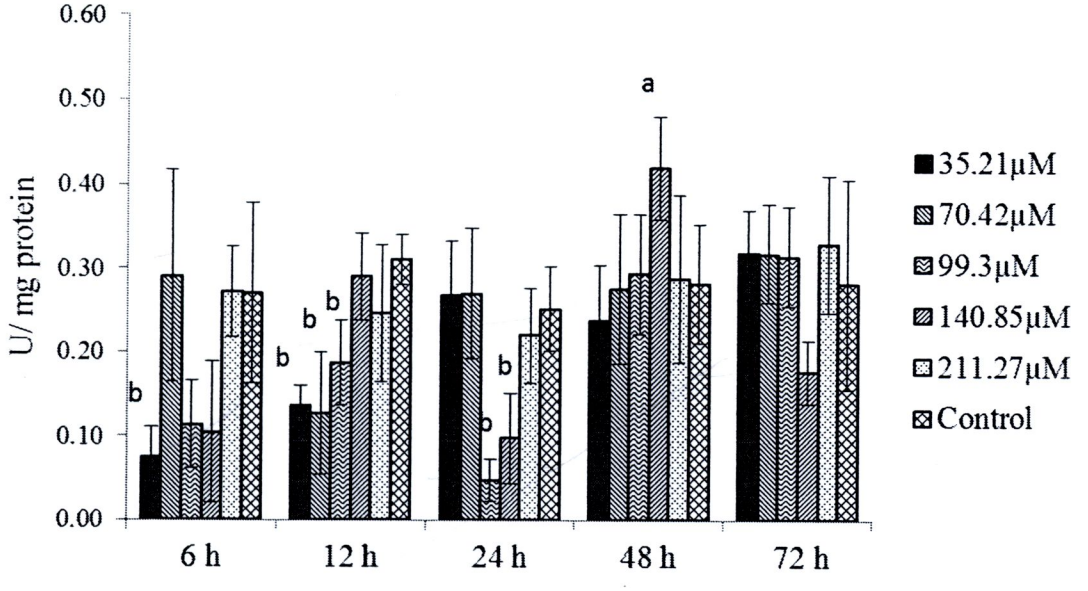

Fig. 4.37. GSTs activity in Hep G2 cells incubated for 6, 12, 24, 48 and 72 h with PEDP. *a* significantly increased ($p < 0.05$) and *b* significantly decreased ($p<0.05$) when compared with the control group.

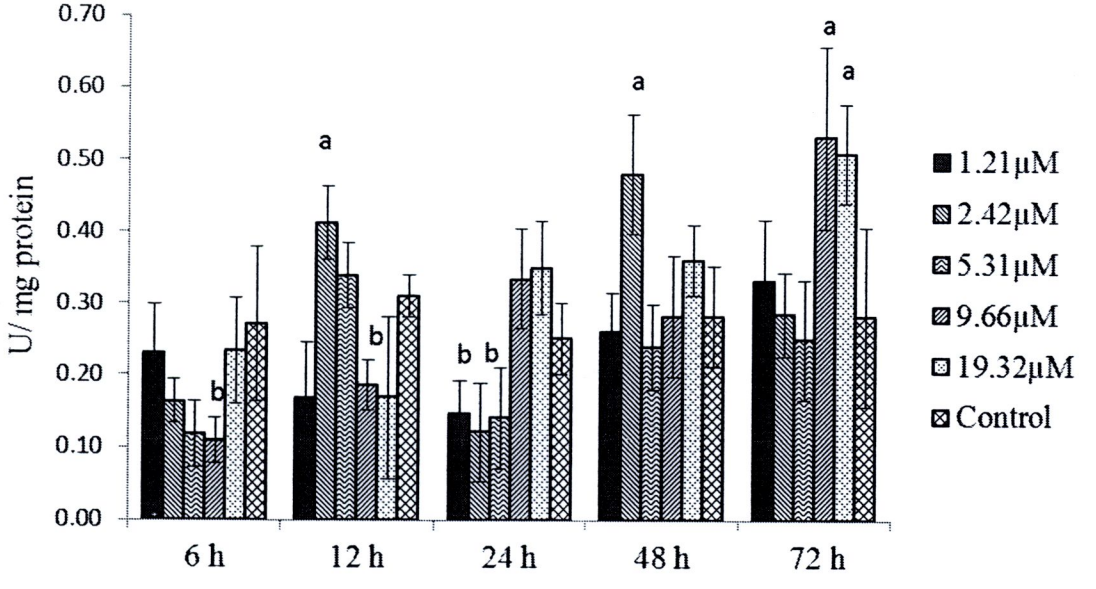

Fig. 4.38. GSTs activity in Hep G2 cells incubated for 6, 12, 24, 48 and 72 h with EDPA. *a* significantly increased ($p < 0.05$) and *b* significantly decreased ($p<0.05$) when compared with the control group.

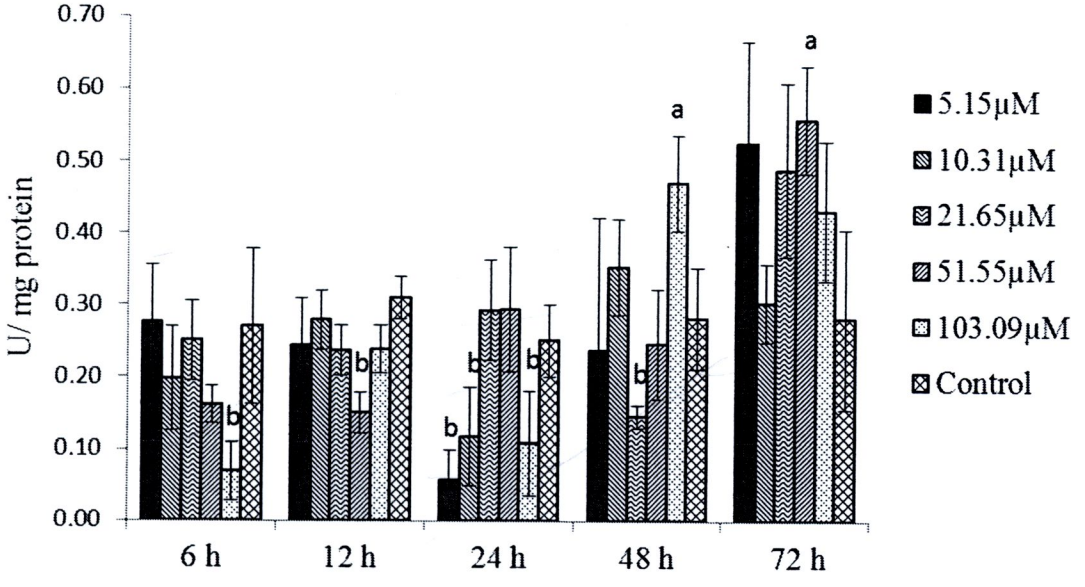

Fig. 4.39 GSTs activity in Hep G2 cells incubated for 6, 12, 24, 48 and 72 h with ODPA. *a* significantly increased ($p< 0.05$) and *b* significantly decreased ($p<0.05$) when compared with the control group.

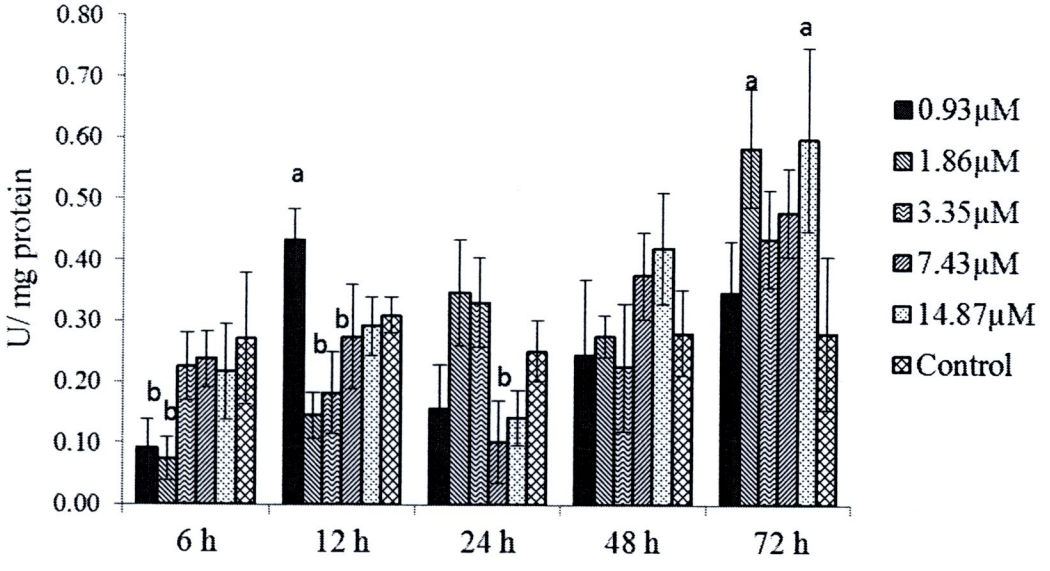

Fig. 4.40 GSTs activity in Hep G2 cells incubated for 6, 12, 24, 48 and 72 h with PMDPA. *a* significantly increased ($p< 0.05$) and *b* significantly decreased ($p<0.05$) when compared with the control group.

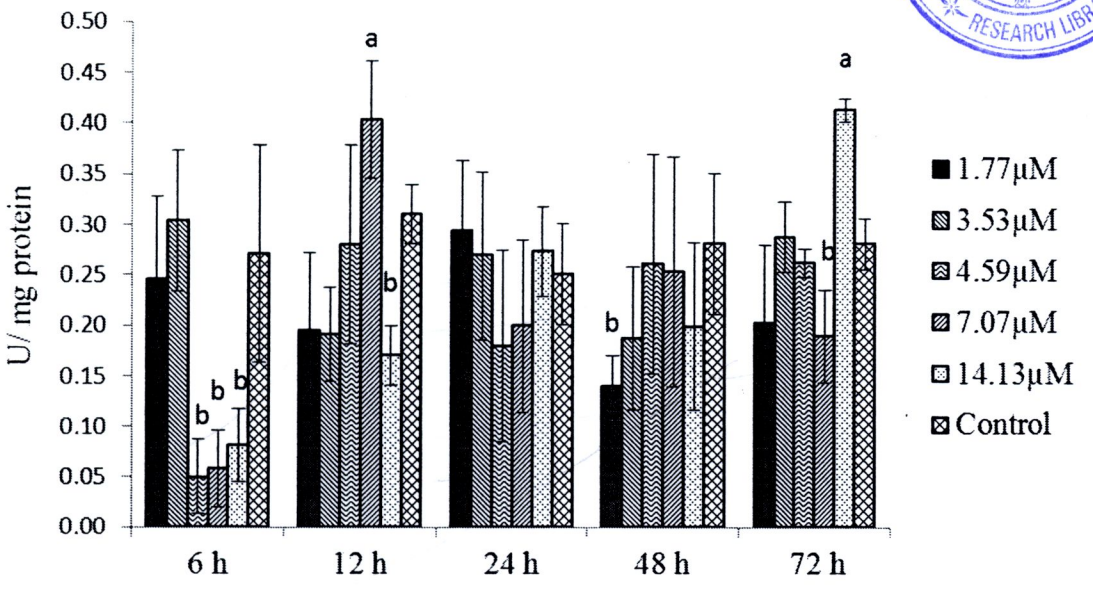

Fig. 4.41. GSTs activity in Hep G2 cells incubated for 6, 12, 24, 48 and 72 h with PEDPA. *a* significantly increased ($p < 0.05$) and *b* significantly decreased ($p<0.05$) when compared with the control group.

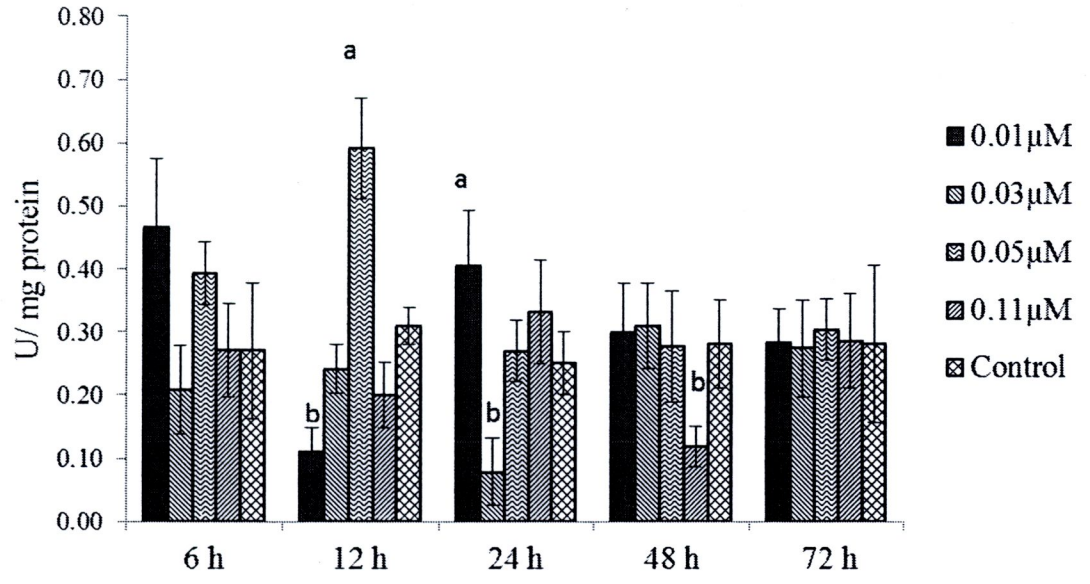

Fig. 4.42. GSTs activity in Hep G2 cells incubated for 6, 12, 24, 48 and 72 h with curcumin. *a* significantly increased ($p < 0.05$) and *b* significantly decreased ($p<0.05$) when compared with the control group.

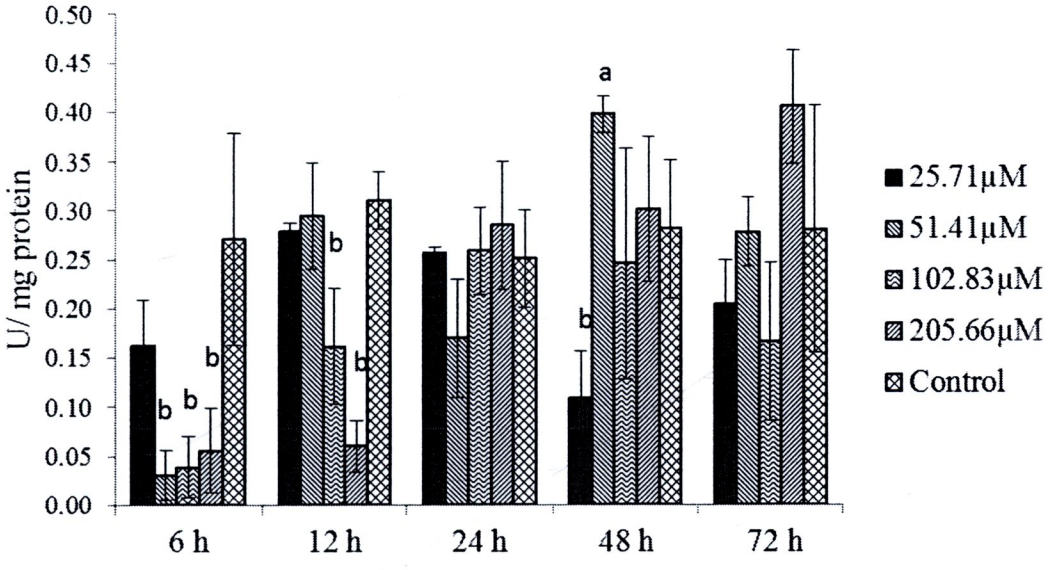

Fig. 4.43. GSTs activity in Hep G2 cells incubated for 6, 12, 24, 48 and 72 h with β-napthoflavone. *a* significantly increased ($p < 0.05$) and *b* significantly decreased ($p<0.05$) when compared with the control group.

4.4.3 Heme oxygenase 1 activity

The method to determine HO-1 activity in this experiment has been shown to give the same results as the more refined mRNA assay that is compatible with mRNA HO-1 expression [115]. After treating the cells with various concentrations of CAF and its derivatives for 6, 12, 24, 48 and 72 h, HO-1 activity was determined by using spectrophotometer.

HO-1 activity was measured after the Hep G2 cells treated with various CAF concentrations. The result is shown in Fig. 4.44. At 12 hour, HO-1 activity decreased when treatment with all concentrations for 12 hour, the HO-1 activities increased when compared with those of control group ($p<0.05$). HO-1 had maximum activity of 120 μM bilirubin/ mg protein /h when treatment with 388 μM of CAF for 48 hour.

Fig. 4.45 shows the effect of EDP on HO-1 activity after treatment HepG2 cells. At time 6 hour, HO-1 had similar activity value. At 12 and 48 hour, 72.12 μM of EDP induced HO-1 activity. After treating the cells with 9.62 μM for 48 hour, HO-1 had maximum activity, 90 μM bilirubin/ mg protein /h. Comparing the activity between treatment groups and control group at 72 hour found that the HO-1 activity of all treatment groups increased ($p<0.05$).

Fig 4.46 shows the effects of ODP on HO-1 activity treating on HepG2 cells. The ODP induced HO-1 activity after treating with 8.56 to 68.49 μM of ODP for 24 and 72 hour. At 6 and 12 hour, HO-1 activities decreased when compared with the control group.

Fig. 4.47 shows HO-1 activity after treating with PMDP. The results showed that treatment with 5.85 to 23.44 μM of PMDP for 6 and 12 hour could decrease HO-

1 activities of the cells. The HO-1 activity had maximum value when treatment with 19.53 μM of PMDP for 48 hour which value as 56 μM bilirubin/ mg protein /h. At 72 hour, HO-1 activity of the cells that treated with 2.95 to 12.11 μM of PMDP increased when compared with the control groups ($p<0.05$).

HepG2 cells were treated with PEDP and determined HO-1 activity and result is shown in Fig 4.48. After treatment the cells with 70.42 and 211.27 μM of PEDP for 6 hour, HO-1 activities significantly increased when compared with the control group ($p<0.05$). At 12 hour, the cells that treated with 140.48 μM of PEDP had maximum HO-1 activity with 67 μM bilirubin/ mg protein /h while, other concentrations decreased HO-1 activities. Treatment the cell for 24 and 72 hour, all doses of PEDP induced HO-1 activity but at 48 hour were decreased activity.

Fig. 4.49 shows the effects of EDPA on HO-1 activity. 12 hour after treatment with 9.66 μM of EDPA, HO-1 activity had maximum value as 98 μM bilirubin/ mg protein /h. HO-1 activity significantly increased after treating with EDPA for 24, 48 and 72 hour.

Fig 4.50 shows the effects of ODPA on HO-1 activity. 6 and 12 hour after treatment with various doses of ODPA while at 72 hour, HO-1 activities were induced when compared with the control groups.

The effect of PMDPA on HO-1 activity is shown in Fig.4.51. Treatment HepG2 cells with 0.93 and 3.35 μM of PMDPA, HO-1 activities were increased comparing with the control groups ($p<0.05$). The maximum value of HO-1 activity was 57 μM bilirubin/ mg protein /h when the cells treated with 0.93 μM of PMDPA

for 12 hour. At 24 and 72 hour after treatment, HO-1 activities increased while at 48 hour; HO-1 activities decreased.

Fig 4.52 shows the effects of PEDPA on HO-1. The results show that the cells treated with 0.93 and 3.35 μM of PEDPA for 6 hour, HO-1 activities were increased. Maximum value of HO-1 was 57 μM bilirubin/ mg protein /h when treatment the cells with 7.07 μM of PEDPA for 12 hour. At 48 and 72 hour, the HO-1 activities were decreased comparing with the control groups ($p<0.05$).

Curcumin and β-napthoflavone were used as positive control. The results are shown in Fig 4.53 and Fig 4.54, respectively. Curcumin induced HO-1 activity with maximum value as 140 μM bilirubin/ mg protein /h when treatment the cells with 0.05 μM of curcumin for 24 hour. Treatment the cells with 51.41 μM of β-napthoflavone induced HO-1 activity as 54 μM bilirubin/ mg protein /h for 48 hour.

All results are shown in Fig. 4.17. HO-1 activities were significantly increased after the compounds were treated for 24 and 48 h when compared with the control. EDP was classified as having the highest activity level (87.3 μM bilirubin/mg protein/h). In this experiment, curcumin and β-napthoflavone were used as the positive control substance. Curcumin and β-napthoflavone had the potential to induce HO-1 activity. The results show that, the times for induction HO-1 activity of small molecules including CAF and EDP, take longer than the large molecules. Ester derivatives were potential induce HO-1 activity than the amide derivatives. CAF and its derivatives enhance OH-1 induction more than β-napthoflavone due to the hydroxyl groups in the *ortho* position on aromatic ring [116]. CAF ester derivatives were hydrolyzed to caffeic acid as the major metabolite [117] and alcohol. HO-1 was

induced in response to alcohol, thiol-containing dietary anti-oxidant, triterpenoid and lipopolysacharide [118]. Treatment with CAF ester derivatives may induce HO-1 activity expression through CAF, alcohol and CAF ester. CAF amides were more stable than CAF esters [15]. Therefore, only the CAF amide compounds might be able to induce HO-1 activity. Those chemicals with hydrophobic properties might easily penetrate cell membranes and induce signal activation. Nrf2 plays a key role in the transcriptional regulation of the HO-1 gene expression through interaction with ARE. Under normal physiologic conditions, Nrf2 is sequestered in the cytoplasm as an inactive complex with its repressor Keap 1. Upon stimulation by inducers, however, Nrf2 dissociates from Keap 1 and translocates into the nucleus where it dimerizes with some cofactors like small Maf protein and binds to ARE. This would lead to activation of a battery of highly specialized proteins, including HO-1 [119]. HO-1 induction by caffeic acid and its derivatives might occur via signaling through the nuclear factor-erythroid-2-related factor Nrf2/ ARE pathway. This hypothesis was supported by CAPE induced HO-1 expression observed in several cell types. The molecular mechanism in the regulation of CAPE mediated HO-1 expression has been studied in some cell types [120]. CAPE disrupts the Nrf2-Keap1 complex, leading to increase Nrf2 binding to ARE. Compounds stimulated nuclear translocation of Nrf2 by inactivating the Nrf2-Keap1complex, which was associated with a significant increase in the activity and HO-1 mRNA [122]. The other caffeic acid derivatives, which have a similar structure to CAPE, may have the same mechanism. It was, therefore, possible that preconditioning Hep G2 cells by caffeic acid and its derivatives may enhance activation of the Nrf2/ARE pathway and induction of phase

II detoxification/antioxidant enzymes upon oxidative stress, thereby resulting in increased resistance to oxidative damage. Mechanisms of HO-1 induction in Hep G2 by caffeic acid and its derivatives will be further investigated.

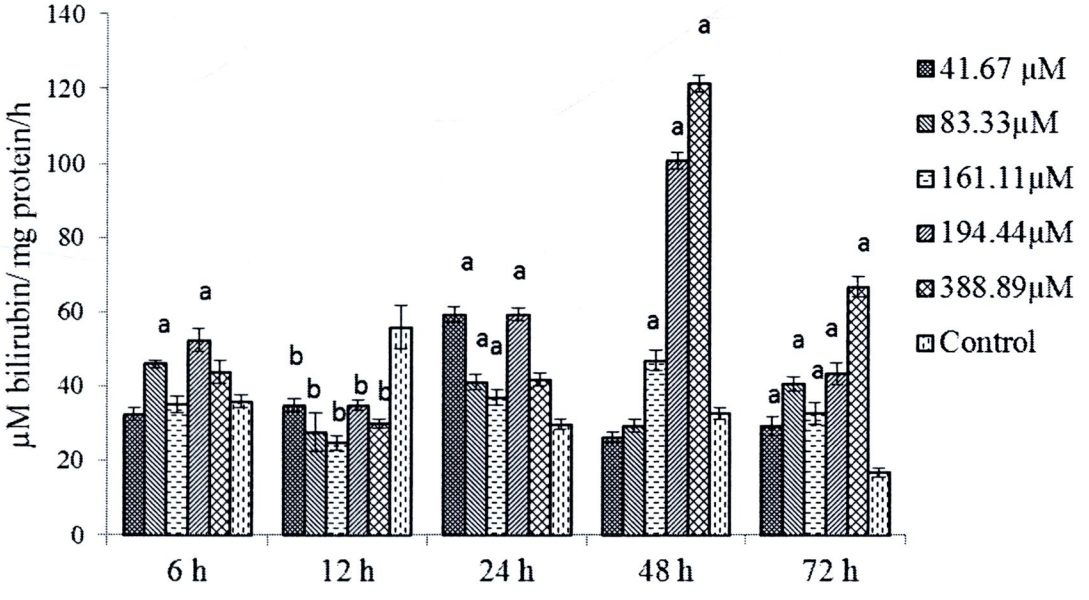

Fig. 4.44 HO-1 activity in Hep G2 cells incubated with CAF. *a* significantly increased, *b* significantly decreased comparing with control group ($p<0.05$).

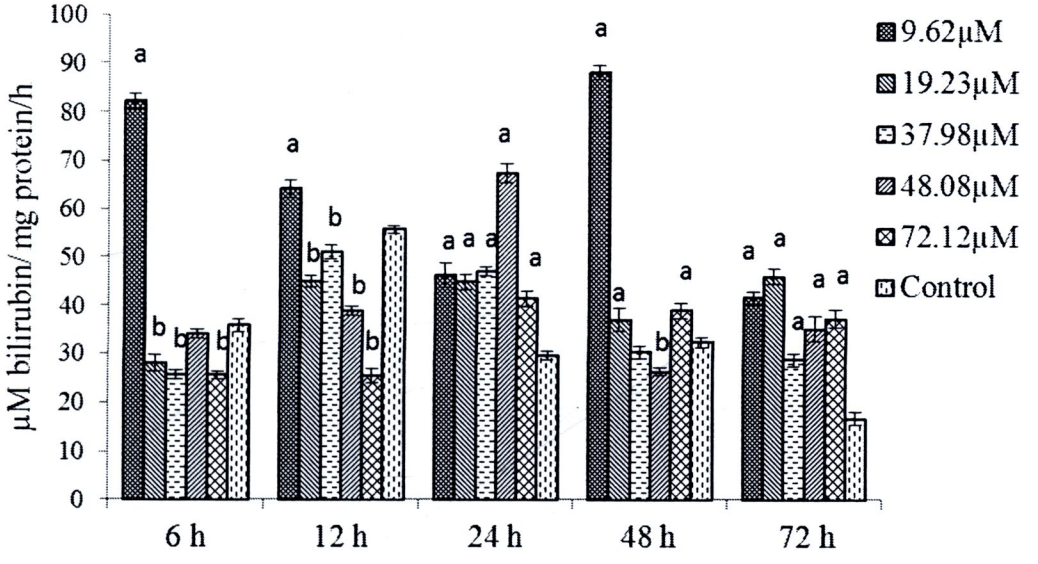

Fig. 4.45 HO-1 activity in Hep G2 cells incubated with EDP. *a* significantly increased, *b* significantly decreased comparing with control group ($p<0.05$)

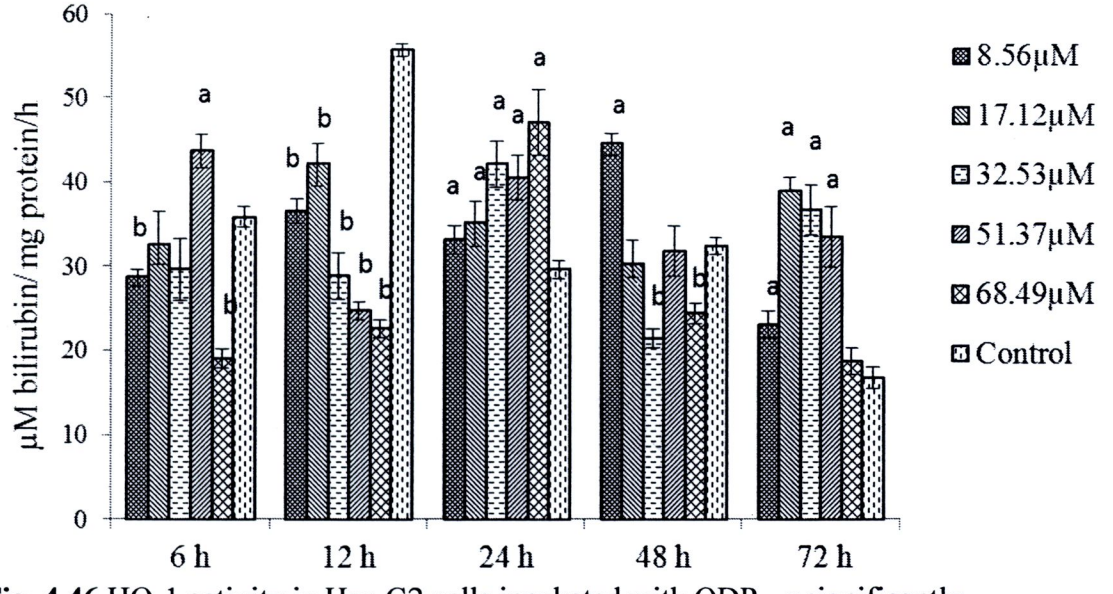

Fig. 4.46 HO-1 activity in Hep G2 cells incubated with ODP. *a* significantly increased, *b* significantly decreased comparing with control group ($p<0.05$).

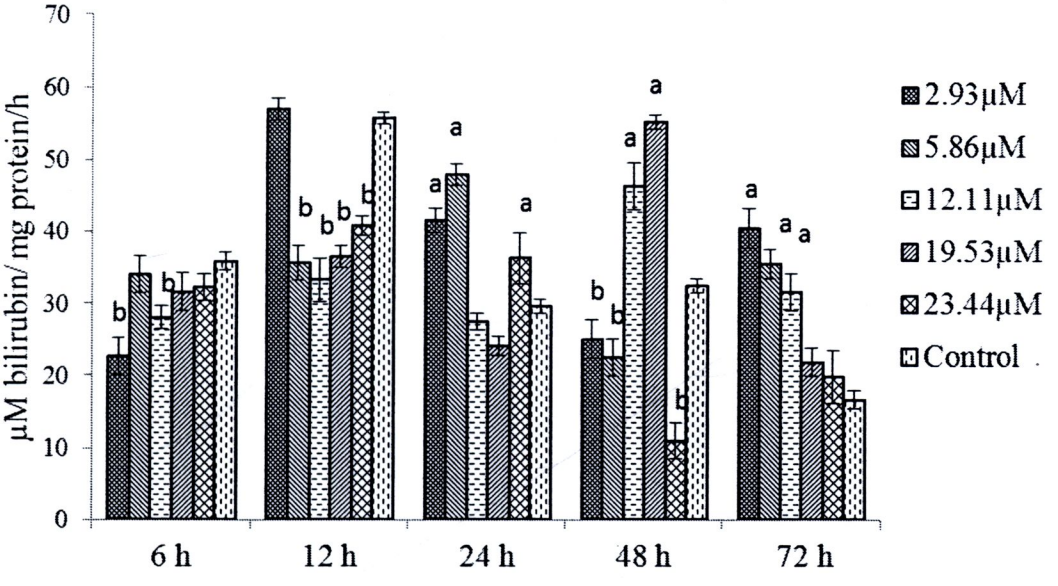

Fig. 4.47 HO-1 activity in Hep G2 cells incubated with PMDP. *a* significantly increased, *b* significantly decreased comparing with control group ($p<0.05$).

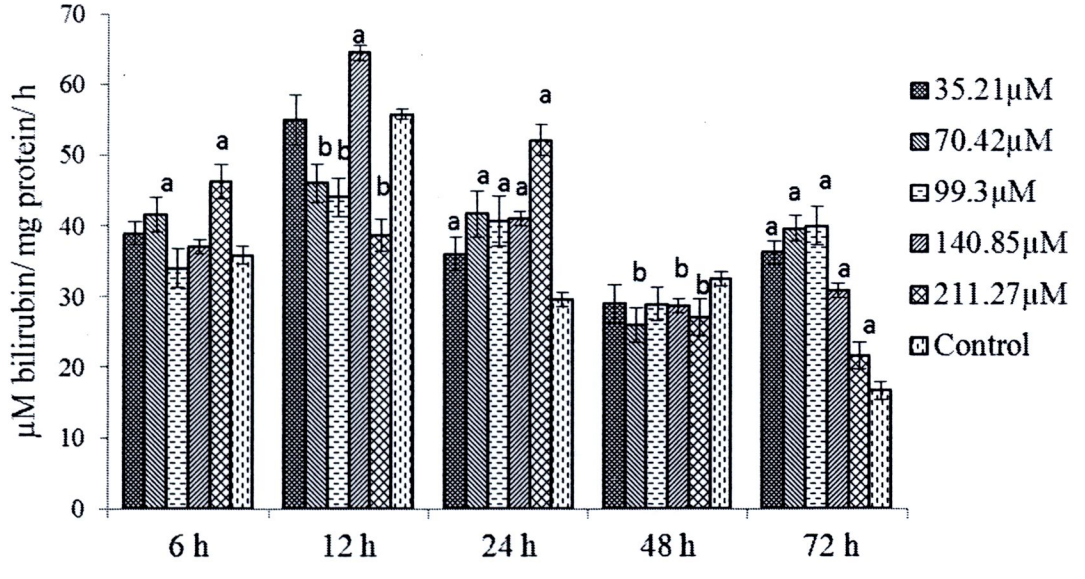

Fig. 4.48 HO-1 activity in Hep G2 cells incubated with PEDP. *a* significantly increased, *b* significantly decreased comparing with control group ($p<0.05$).

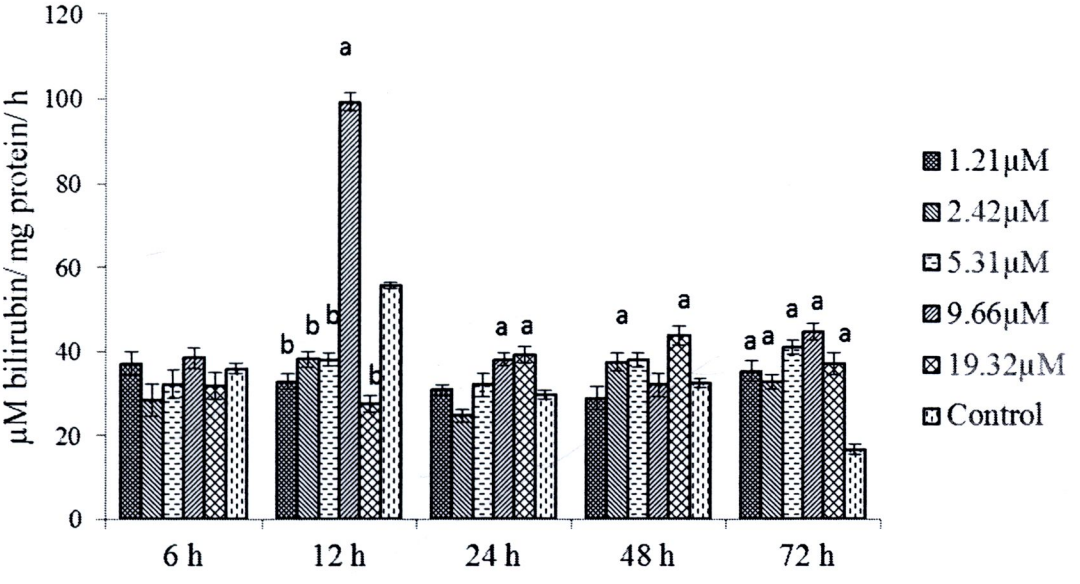

Fig. 4.49 HO-1 activity in Hep G2 cells incubated with EDPA. *a* significantly increased, *b* significantly decreased comparing with control group ($p<0.05$).

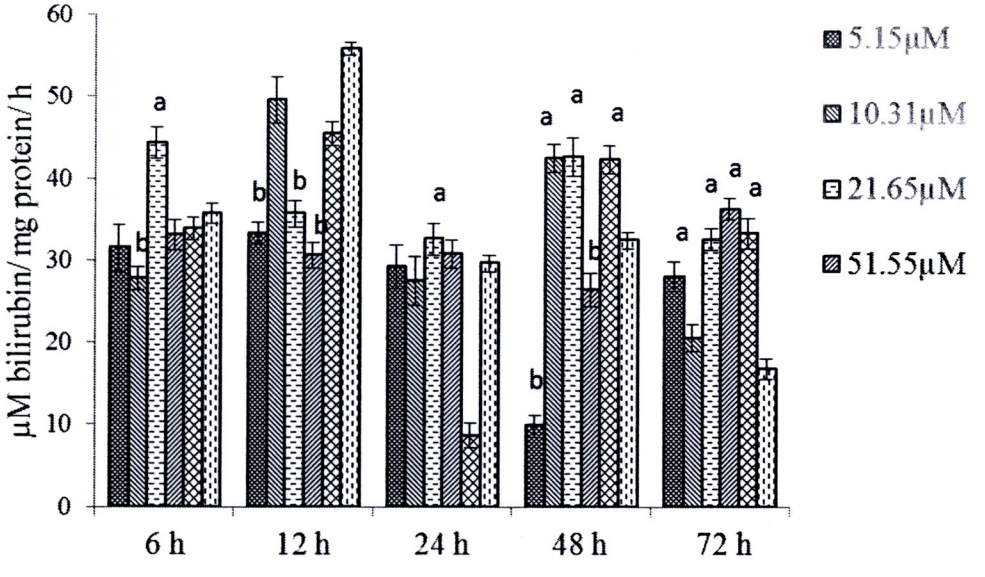

Fig. 4.50 HO-1 activity in Hep G2 cells incubated with ODPA. *a* significantly increased, *b* significantly decreased comparing with control group ($p<0.05$).

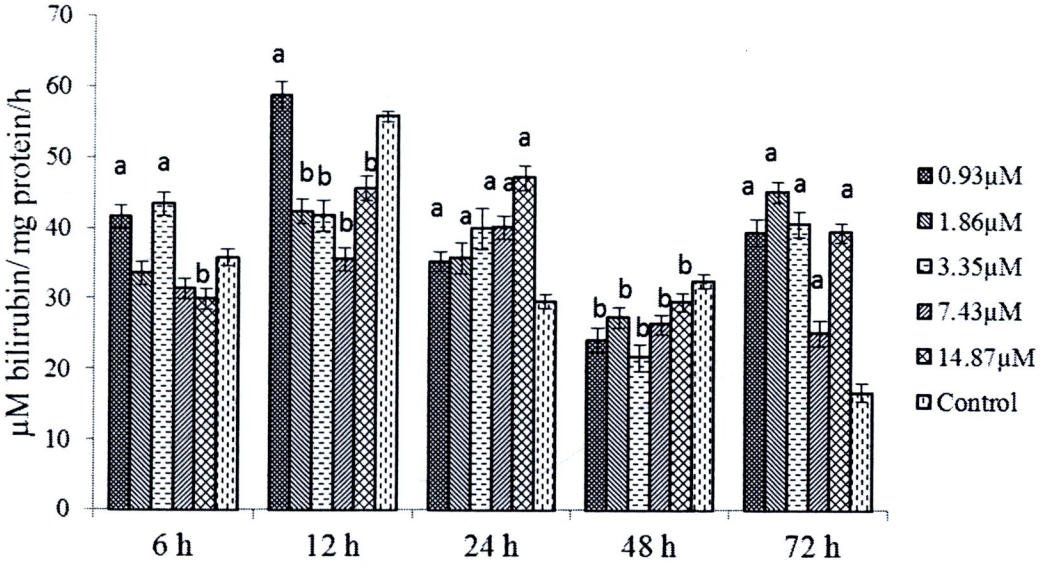

Fig. 4.51 HO-1 activity in Hep G2 cells incubated with PMDPA *a* significantly increased, *b* significantly decreased comparing with control group ($p<0.05$)

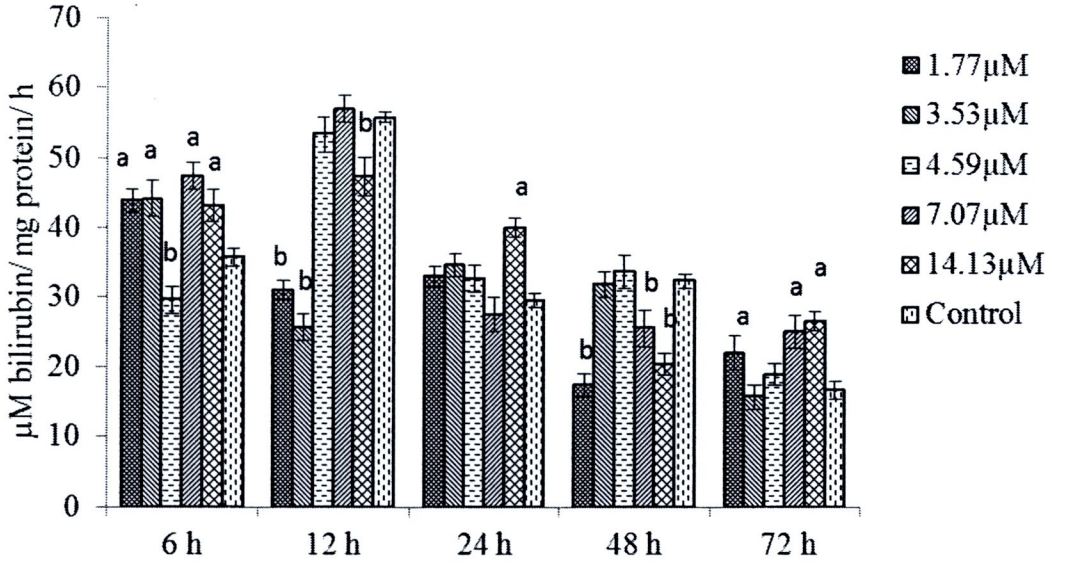

Fig. 4.52 HO-1 activity in Hep G2 cells incubated with PEDPA. *a* significantly increased, *b* significantly decreased comparing with control group ($p<0.05$).

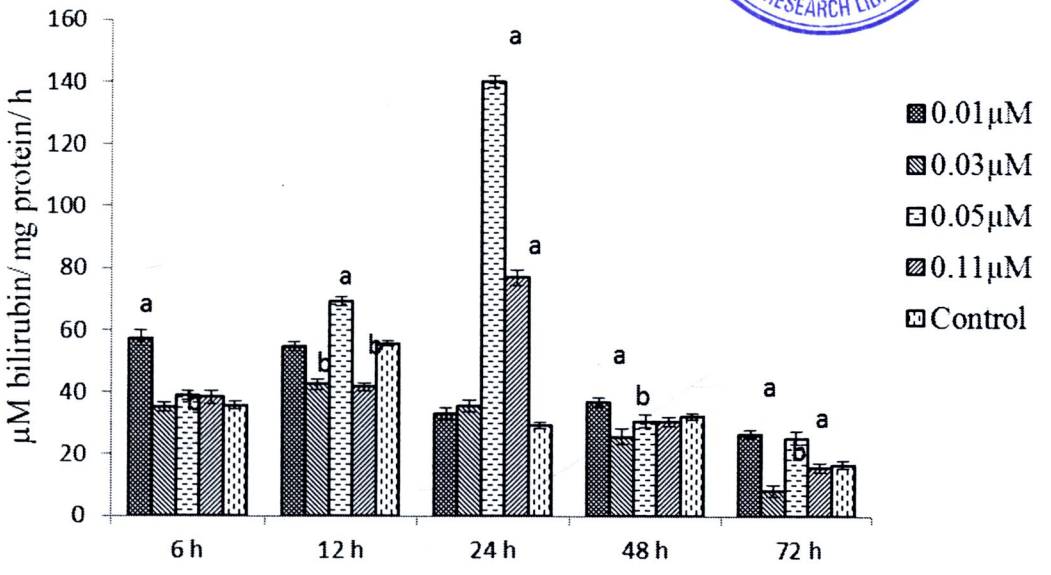

Fig. 4.53 HO-1 activity in Hep G2 cells incubated with curcumin. *a* significantly increased, *b* significantly decreased comparing with control group ($p<0.05$).

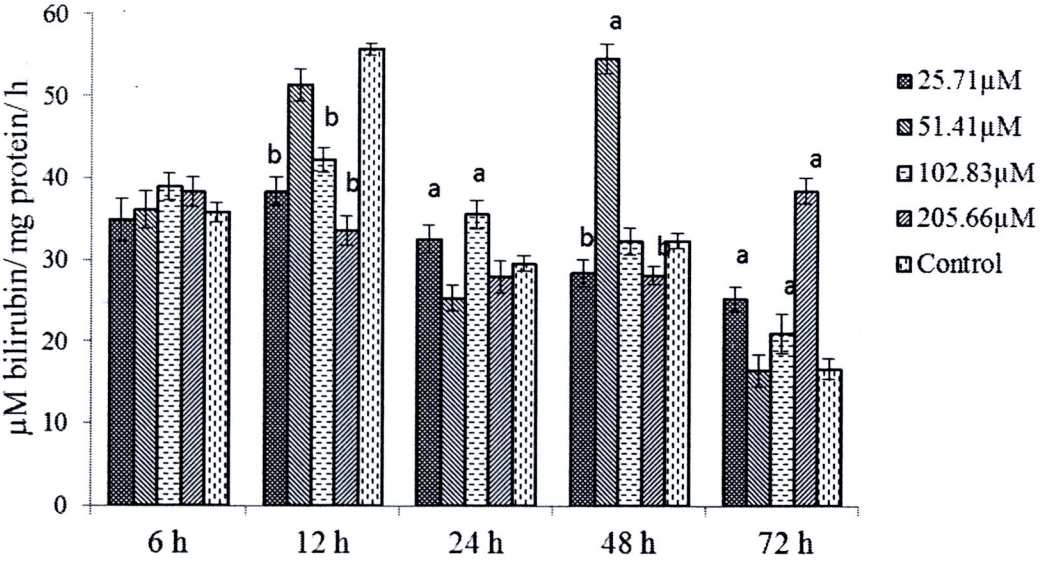

Fig. 4.54 HO-1 activity in Hep G2 cells incubated with β-napthoflavone. *a* significantly increased, *b* significantly decreased comparing control group ($p<0.05$).

4.5. Cytotoxicity of Hep G2 cell line.

The MTT assay was used to evaluate the cytotoxic effect of CAF and its derivatives on Hep G2 cells. Cells were exposed to various concentrations of CAF and its derivatives for specific periods and viability was assayed. Fig. 4.55 shows the viable cells number decreased as the concentration of CAF or its derivatives increased, suggesting that CAF and its derivatives induced HepG2 cells death in a concentration-dependent manner. The IC_{50} values of PMEDP, EDPA, PMDP, PEDPA, EDP, ODP, ODPA, CAF and PEDP were 37.80, 41.27, 41.47, 54.80, 105.50, 132.05, 398.43, 648.85 and 681.85 μM, respectively. From the table, it seems that both ester and amide derivatives strongly inhibited the growth of Hep G2 cells line better than CAF. The IC50 values ranged from 41.27-648.85 μM. Among them, EDPA seemed to possess the highest potency to inhibit liver cancer cell growth, 15.7 times of CAF. Moreover, amide derivatives seem to exert high potential to inhibit cell viability than ester derivatives. Many researchs showed the mechanism of CAF and caffeic acid phenethyl ester in many types of cancer cells by apoptosis [123]. CAF- induced apoptosis by inhibiting Bcl-2 activity, leading to release of cytochrome c and subsequent activation of casspace-3, indicating that CAF induced apoptosis via the mitochondrial apoptotic pathway [124]. Ujibe and co-worker reported that octyl caffeate induced apoptosis in human leukemia U937 cells [125].

This experiment may extrapolated that CAF and its derivatives might induce Hep G2 apoptosis via inhibit NF-kB and inhibit Bcl-2 activity. Apoptosis of tumor cells can be triggered by various treatments such as irradiation, Fas (a cell surface molecule mediating apoptosis) ligand and antitumor drugs. The regulation of

apoptosis requires two major protein families, Bcl-2 related gene products and caspaces. The growing Bcl-2 protein family contains several homologous proteins including antiapoptotic proteins (Bcl-2, Bcl-xL) and proapoptotic proteins (Bax, Bad). CAPE induces apoptosis in certain tumor cells; its action is accompanied by the activation of caspase-3, down-regulation of Bcl-2 and up-regulation of Bax. Apoptosis via numerous triggers including the binding of ligands to death receptors is antagonized by the activation of NF-kB and potentiated by its inhibition. Moreover, CAPE activates the Fas death receptor. Further studies are nassary to evaluate the mechanism in the induction of apoptosis by CAF the others CAF derivatives.

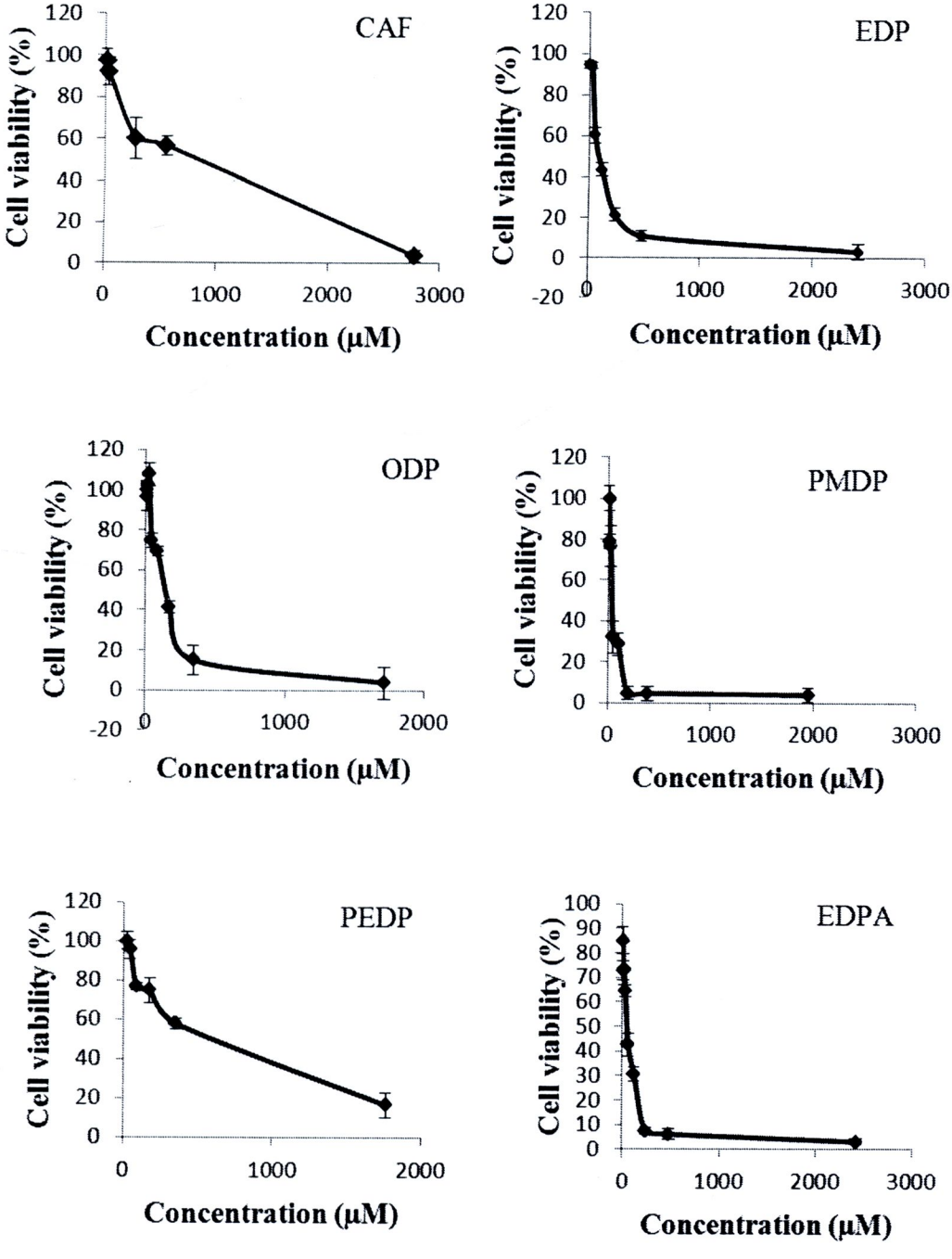

Fig 4.55 Dose-dependent cytotoxicity of CAF and its derivatives.

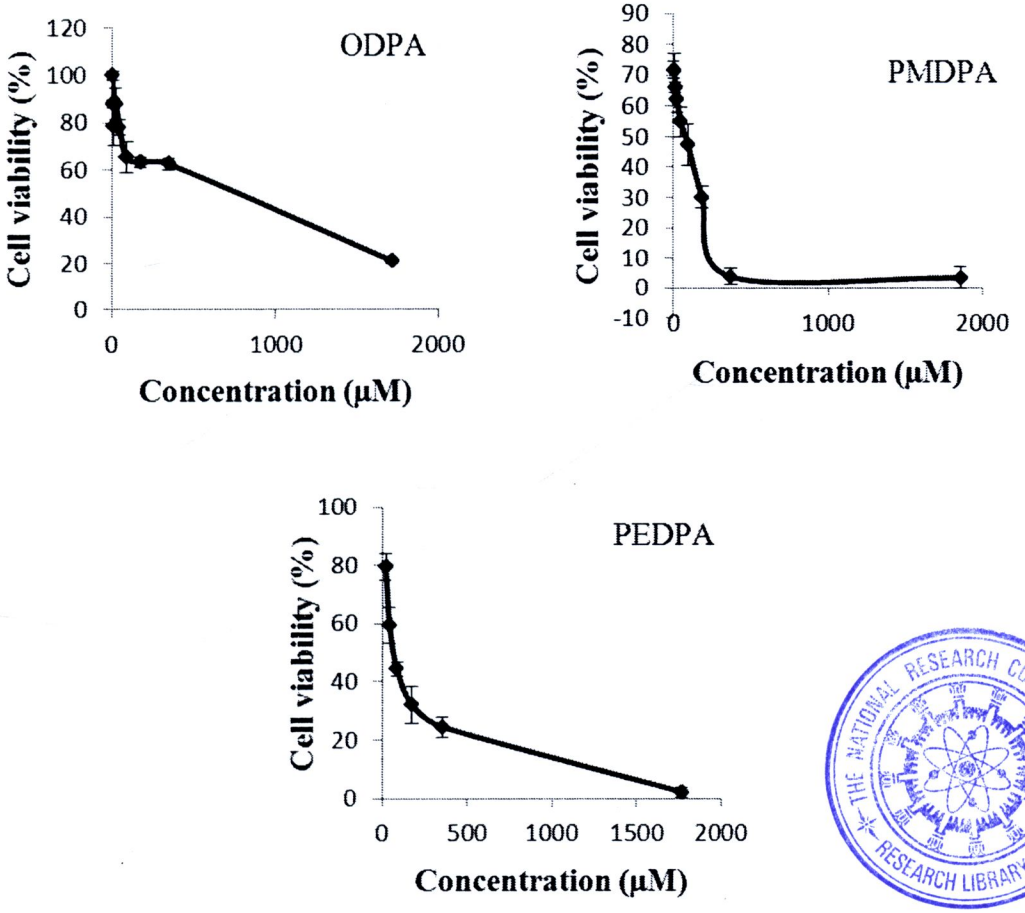

Fig. 4.55(con't) Dose-dependent cytotoxicity of CAF and its derivatives.